Development

Differential Effects of the G-Protein-Coupled Estrogen Receptor (GPER) on Rat Embryonic (E18) Hippocampal and Cortical Neurons

Kyle Pemberton,[1,2,*] Martina Rosato,[1,2,*] Cass Dedert,[1,2] Chelsea DeLeon,[4] Christopher Arnatt,[2,3,4] and Fenglian Xu[1,2,3]

https://doi.org/10.1523/ENEURO.0475-21.2022

[1]The Department of Biology, College of Arts and Sciences, Saint Louis University, St. Louis, MO 63103, [2]The Henry and Amelia Nasrallah Center for Neuroscience, Saint Louis University, St. Louis, MO 63104, [3]The Department of Pharmacology and Physiology, School of Medicine, Saint Louis University, St. Louis, MO 63104, and [4]The Department of Chemistry, College of Arts and Sciences, Saint Louis University, St. Louis, MO 63103

Abstract

Estrogen plays fundamental roles in nervous system development and function. Traditional studies examining the effect of estrogen in the brain have focused on the nuclear estrogen receptors (ERs), ERα and ERβ. Studies related to the extranuclear, membrane-bound G-protein-coupled ER (GPER/GPR30) have revealed a neuroprotective role for GPER in mature neurons. In this study, we investigated the differential effects of GPER activation in primary rat embryonic day 18 (E18) hippocampal and cortical neurons. Microscopy imaging, multielectrode array (MEA), and Ca^{2+} imaging experiments revealed that GPER activation with selective agonist, G-1, and nonselective agonist, 17β-estradiol (E2), increased neural growth, neural firing activity, and intracellular Ca^{2+} more profoundly in hippocampal neurons than in cortical neurons. The GPER-mediated Ca^{2+} rise in hippocampal neurons involves internal Ca^{2+} store release via activation of phospholipase C (PLC) and extracellular entry via Ca^{2+} channels. Immunocytochemistry results revealed no observable difference in GPER expression/localization in neurons, yet real-time qPCR (RT-qPCR) and Western blotting showed a higher GPER expression in the cortex than hippocampus, implying that GPER expression level may not fully account for its robust physiological effects in hippocampal neurons. We used RNA sequencing data to identify distinctly enriched pathways and significantly expressed genes in response to G-1 or E2 in cultured rat E18 hippocampal and cortical neurons. In summary, the identification of differential effects of GPER activation on hippocampal and cortical neurons in the brain and the determination of key genes and molecular pathways are instrumental toward an understanding of estrogen's action in early neuronal development.

Key words: electrophysiology; estrogen; G-protein-coupled estrogen receptor (GPER/GPR30); hippocampus; neurodevelopment; transcriptome

---

Significance Statement

Studies of estrogen function via a non-nuclear G-protein-coupled estrogen receptor (GPER/GPR30) in the brain have primarily focused on mature neurons and neuroprotective actions with little investigation into the role of GPER in early neural development. In this work, we discover differential effects of GPER on early neurite outgrowth, neuronal activity, and intracellular calcium (Ca^{2+}) signaling in primarily cultured rat embryonic [embryonic day (E)18] hippocampal and cortical neurons. This study further highlights distinct, transcriptomic genes and pathways that are regulated by GPER agonists in early developing hippocampal and cortical neurons. These results advance our fundamental understanding of estrogen functions via GPER signaling in different (hippocampal vs cortical) neurons during early neuronal development. This knowledge is also instrumental for therapeutics for GPER-related neurodevelopmental disorders.

Introduction

The steroid hormone estrogen plays crucial roles in the nervous system, ranging from developmental function to neuroprotection after injury (Miranda et al., 1994; Kajta and Beyer, 2003). The observed physiological actions of 17β-estradiol (E2), the most active form of estrogen, were originally attributed to the classical, nuclear estrogen receptors (ERs) ERα (P. Walter et al., 1985; Green et al., 1986) and ERβ (Kuiper et al., 1996). Since then, cloning of the orphan G-protein-coupled receptor (GPCR), *GPR30/GPER-1* (Carmeci et al., 1997; Kvingedal and Smeland, 1997), and subsequent deorphanization with estrogen have led to the identification of the G-protein-coupled ER (GPER; Filardo et al., 2002; Revankar et al., 2005). GPER is ubiquitously expressed in the rat brain (Brailoiu et al., 2007; Hazell et al., 2009) with a higher level of expression in the hippocampus, cortex, and hypothalamus compared with other brain regions (Hazell et al., 2009). Additionally, recent transcriptomics of adult rats has shown that the GPER transcript predominates in the brain compared with other tissues and exhibits a higher level of expression compared with the classical ERs (Hutson et al., 2019). These findings further suggest that a physiological role for GPER in the brain exists.

Despite knowledge of the importance of estrogen on the developing nervous system, direct evidence related to the role of GPER in early neuronal development is limited. Currently, research has focused on the role of GPER in mature neuronal function, primarily related to estrogen's protective role in diseases such as Parkinson's disease (Bourque et al., 2015; Côté et al., 2015) and ischemic stroke (Murata et al., 2013; Broughton et al., 2014). In addition, emerging research suggests that GPER may contribute to the etiology of neurodevelopmental and neuropsychiatric disorders, including autism spectrum disorder (Altun et al., 2017), schizophrenia (Gogos et al., 2015), attention deficit hyperactivity disorder (Sahin et al., 2018), anxiety (Li et al., 2013; Tian et al., 2013), and depression (McAllister et al., 2012, 2014). Moreover, the identification of *GPER-1* polymorphisms and evidence that variants of GPER may result

in miscarriage during pregnancy (Tang et al., 2017) suggest that GPER plays an important role in fetal development. Further research performed in zebrafish embryos has shown a high expression of GPER in the nervous system during development (Shi et al., 2013), although the activity and mechanism have yet to be established.

The role of estrogen may not be stagnant and critical periods during development may influence gene expression. Estrogen and estrogen precursor levels in the hippocampus and cortex of rats decrease after E19 and continue to attenuate postnatally (Konkle and McCarthy, 2011), suggesting that estrogens play an important role in early neuronal development. In addition, estrogen can be produced locally in multiple brain regions in rats, including the hippocampus and cortex, and functions as a bona fide neurotrophic and neuromodulatory factor that increases synaptic plasticity within minutes to hours (Srivastava et al., 2008). Research on the pharmacology and signaling associated with GPER modulation within the brain is not well understood and may depend on the cell population (Beyer et al., 2002). For example, in adult rat cortex GPER activation induces calcium (Ca^{2+}) signaling in astrocytes but not neurons (Roque and Baltazar, 2019; Roque et al., 2019). Despite these findings, few studies have focused on the effect of GPER in rat brains during early developmental stages, such as Embryonic day 18 (E18) neurons. To help fill this gap, we sought to uncover the effects of GPER during early neuronal development in rat E18 neurons originating from the hippocampus and cortex. Differential effects of targeting GPER in the hippocampus and cortex were observed with E2 and the GPER-specific agonist, G-1. The hallmark observation measured for neuronal development in our study was neurite outgrowth. We found that GPER promotes neurite outgrowth in hippocampal but not cortical neurons. Our results further revealed different physiological and signaling events between hippocampal and cortical neurons. In particular, hippocampal neurons showed greater action potential firing (neuronal activity) and intracellular Ca^{2+} oscillations than cortical neurons in response to GPER activation. These differences in physiological and signaling effects may not be attributed to the level of GPER expression. Instead, these differences may depend on more profound regulation of specific genes and signaling pathways in hippocampal cultures. RNA sequencing was used to interrogate changes in gene regulation in response to GPER activation and identify specific signaling pathways. These results are crucial in understanding the targetability of GPER during early neuronal development.

Materials and Methods

Animals and neuronal cell culture

Animal maintenance and experiments were conducted using protocols that follow the guidelines outlined by the National Institute of Health Animal Use Guidelines and were performed in accordance with Saint Louis University Animal Care and Use Committee. All experiments were conducted on primary neurons derived from the brains of E18 rat pups. The sex of the embryos was not determined

because E18 is before the critical period (McCarthy, 2016) for masculinization, in which the testes in males begin producing large amounts of testosterone. Using neurons that have yet to be exposed to this masculinization process allows us to have confidence that sex-specific differences have not occurred and should not give confounding results based on the sex of the pups and the cells that were harvested from them.

Rat E18 primary neurons were cultured using standard dissection and culturing protocols (Pacifici and Peruzzi, 2012) in charcoal-stripped serum and phenol red-free neurobasal medium (Invitrogen, catalog #12348017) to ensure the absence of hormones or estrogenic components in medium. In short, pregnant dams were killed using CO_2, and E18 pups were quickly removed by C-section. The brains were removed, and hippocampi and cortices were separated and placed in cold HBSS without phenol red (Invitrogen, catalog #14025092). Once all hippocampi and cortices were isolated, they were suspended separately in 50 units/ml papain solution in a 5% CO_2, 37°C, humidified incubator for 25 min, mixing gently every 5 min. The enzyme was washed away with serum-containing medium and the tissues were mechanically triturated using flame-polished glass pipettes with progressively smaller openings. Cells were resuspended in culture medium containing neurobasal medium without phenol red, 1% L-glutamine or 1× GlutaMax (Invitrogen, catalog #35050061), 1% pen-strep, 1× B-27 supplement (Invitrogen, catalog #17504044), and 4% charcoal-stripped fetal bovine serum (FBS). Cells were then plated on glass-bottom culture dishes (MatTek, catalog #P35G-0-10-C), multichamber slides with removable wells (MatTek, catalog #CCS-8), multichamber cover glass slides (ThermoFisher, catalog #155411), or multielectrode array plates (Multichannel Systems, catalog #60MEA200/30iR-Ti) precoated with 100 µg/ml poly-D-lysine and 2 µg/ml laminin and incubated in a 5% CO_2, 37°C, humidified incubator. To minimize glial proliferation without introducing unnecessary toxicity of an antimetabolic agent such as Ara-C, the medium was replaced with serum-free culture medium without pen-strep after 24 h in culture (HIC). The removal of pen-strep is because of findings that antibiotics can cause changes in gene expression (Ryu et al., 2017) as well as altering signaling in neurons (Bahrami and Janahmadi, 2013). The culturing surface was coated by applying a solution of 100 µg/ml poly-D-lysine and 2 µg/ml laminin in PBS to the entire culturing surface for 1 h at room temperature and then washed 3× with sterile water. Cultures were labeled with letter and number designations for blinding. Images and files were saved with the letter/number designation and not identified by treatment until analysis was completed.

Neurite outgrowth and ImageJ neurite tracing and analysis

Comparisons between hippocampal and cortical neurons were conducted by culturing rat cortical neurons and hippocampal neurons separately at 200–300 cells/mm^2 with 0.1% DMSO (vehicle), G-1 (100 nM), G-1 + G-15 (10 nM), E2 (100 nM), and E2 + G-15. Cultures from each group were fixed after 8, 20, 48, 72, and 96 HIC and images were taken on an Olympus IX73 inverted microscope equipped with a Retiga R1 camera (QImaging Corporation) and acquired with Micro-Manager (µManager; Edelstein et al., 2010). Concentrations of GPER agonists and antagonists are based on pharmacological profiles of agonism and antagonism according to well-established literature. Specifically, compound G-15 shows no appreciable binding to $ER\alpha$ or $ER\beta$ at concentrations below 10 µM (Dennis et al., 2011). Similarly, competition binding assays revealed no appreciable binding of G-1 to $ER\alpha$ and $ER\beta$ at concentrations up to 1 µM (Bologa et al., 2006). Therefore, we chose to use G-1 at 1–100 nM and G-15 at 10 nM; both concentrations are determined to be specific to GPER binding only.

Neurite measurements were obtained using the ImageJ package Fiji (Schindelin et al., 2012) as previously described (Imaninezhad et al., 2018; Pemberton et al., 2018; Mersman et al., 2020). In short, images were adjusted by subtracting the background to allow the processes to be more easily visualized by using the Subtract Background tool. Once backgrounds were subtracted, neurite growths were traced and labeled by cellular origin using the NeuronJ plugin (Meijering et al., 2004). Any outgrowth that was <5 µm was removed. The remaining outgrowths were labeled by their origin and summed to generate the total outgrowth per cell in R Studio (Rstudio, 2015). Neurite lengths are represented by the average total length of processes per cell as previously described (Beyer et al., 2002).

Multielectrode array (MEA) recording of neuronal activity

Neurons were cultured on MEAs (containing electrodes in an 8 × 8 pattern) at a density of 400–500 cells/mm^2 for a period of 14–18 d for acceptable numbers of synaptic contacts to occur (Basarsky et al., 1994; Dehorter et al., 2012). Measurements were taken for 5–10 min per sample at 20 kHz using the MEA2100-Lite headstage (Multi Channel Systems) connected to an MCS-IFB interface board. The temperature was kept at 37°C using a TC 01 temperature controller. Multi Channel Experimenter software was used to record measurements and activity spikes were identified using Multi Channel Analyzer, then exported into CSV format using Multi Channel Data Manager for further analysis. The activity was determined in R by finding the number of spikes per minute recorded by the electrode. To account for MEAs measuring activity in an area that may have a more or less dense population of cells than other electrode populations, each electrode's activity was normalized to the activity of the electrode before treatment. Activity between treatments was compared by assessing the average amount of spikes in electrical activity per minute. The reported n numbers for these experiments represents the total number of active electrodes in each treatment group from at least three culturing experiments. Cells used for each culture were dissociated from hippocampi and cortices collected from the brains of three to six animals in each experiment.

Ca^{2+} imaging

Primary cells cultured for 11–15 d at a density of 400–500 cells/mm^2 were incubated in 5 μM fura-2 AM (ThermoFisher Scientific catalog #F1201) Ca^{2+} dye in HBSS without phenol red (Invitrogen, catalog #14025092) for 1 h in a 37°C incubator. Cells were then washed four times (10 min per wash) in HBSS at room temperature. Once washed, cells sat for 15–30 min on the imaging rig (Olympus IX73 inverted microscope) to allow the temperature to equilibrate and for full de-esterification of the fura-2 AM. Samples using any antagonists or pharmacological blockers (e.g., G-15, U73122, etc.) had the antagonists/blockers added after the final wash of fura-2 AM and incubated for 30 min (i.e., pretreated for ~30 min) before being mounted on the imaging rig. The basal Ca^{2+} level in vehicle or antagonists/blockers alone was first recorded for ~5 min before adding agonists in the continued presence of antagonists/blockers. Fura-2 was excited sequentially at 340- and 380-nm wavelengths delivered from λ XL equipped with a high-speed wavelength switcher (Sutter Instrument) via an Olympus 40× objective. The emitted fluorescence signal was collected at 510 nm by a Retiga R1 camera (QImaging). The ratio of fluorescence signal at 340 and 380 nm was obtained using the MetaFluor Imaging software (Molecular Devices) at 0.5–1 Hz and analyzed using ImageJ. At the end of each experiment, 40 mM KCl, a standard neuron stimulator, was applied to the cells. Cells responding to KCl with Ca^{2+} rise were confirmed to be neurons and are included for analysis. Failing to respond to KCl indicates the cells are either not healthy or not neurons and were not included in the analysis.

The images obtained were used to create a region of interest (ROI) around each neuron based on cell morphology. A background ROI was made separately in an empty region of the images. An ImageJ macro was developed to import each channel as an image stack to subtract the background for each image, get the average pixel intensity of each ROI, and save these values in a separate file for each channel. Results of the ImageJ macro were then imported into R to analyze the ratio between the two channels. First, the two channels' results were imported into R and normalized. Where Ca^{2+} peaks were analyzed, peaks were determined using a modified version of the NeuronActivityTool's (Prada et al., 2018) peak identification code. The δ (Δ) levels of rise in Ca^{2+} by agonists were shown in figures, which measured the difference in mean peak amplitudes of Ca^{2+} (340/380 ratio) in the presence of agonists + antagonists/blockers as compared with the initial basal Ca^{2+} level in the presence of antagonists/blockers alone.

Immunocytochemistry

The expression and localization of GPER in hippocampal and cortical neurons were monitored using immunofluorescent staining and confocal microscopy techniques. Specifically, rat hippocampal and cortical neurons were cultured separately at 200–300 cells/mm^2 for 72 HIC. Neurons were then fixed with 4% paraformaldehyde (PFA) for 20 min and permeabilized with 0.3% Triton-X in 1× PBS for 5 min at room temperature (21–22°C). Cells were washed twice with 1× PBS and incubated for 1 h in blocking solution (5% goat serum in 1× PBS). After 1 h, blocking solution was replaced with monoclonal mouse anti-microtubule-associated protein 2 (MAP2; Invitrogen, catalog #13-1500, neuronal marker) and polyclonal rabbit anti-GPER (Invitrogen, catalog #PA5-28647) antibodies diluted in blocking solution (1:200) and incubated overnight at 4°C. The primary antibodies were removed and cells were washed three times in 1× PBS for 10 min each. Fluorescently-tagged secondary antibodies Alexa Fluor 488 goat anti-mouse (ThermoFisher, catalog #A-11029) and Alexa Fluor 568 goat anti-rabbit (ThermoFisher, catalog #A-11011) diluted in blocking solution (1:500) were added and allowed to incubate for 1 h at room temperature. Secondary antibodies were then aspirated and cells were washed three times in 1× PBS then once in DI H$_2$O. Cells were then mounted using Fluoroshield with DAPI (Sigma-Aldrich, catalog #F6507). Fluorescent images were taken using a confocal microscope (Leica TCS SP8), then processed and analyzed using ImageJ. The specificity of GPER and MAP2 antibodies was confirmed by staining neurons when either primary or secondary antibody was excluded from the incubation medium. Extended Data Figure 7-1A shows the results, which demonstrate that a fluorescence signal was only detected when both primary and secondary antibodies were included in the staining procedure. To verify whether neurons exhibited autofluorescence, the cells were excited with all lasers (568, 488, and 403 nm) of the confocal microscope and no autofluorescence was observed (data not shown).

Western blotting

For immunoblotting, bilateral hippocampi and cortices were collected from individual brains of E18 embryos ($n = 10$ from three independent preparations). Tissues were treated with Laemmli sample buffer (Bio-Rad, catalog #1610611) containing 350 mM DTT (Bio-Rad, catalog #1610747) and run on a precast MES-SDS gel (NuPage, catalog #NP0323BOX) in a Novex Mini-Cell device (Invitrogen, catalog #EI0001). Bands were transfered to a 0.45 μm nitrocellulose membrane (Bio-Rad, catalog #1620115) in a Mini Protean Tetra System (Bio-Rad, catalog #1658004). Membranes were blotted using primary antibodies for GPER (Invitrogen, catalog #PA5-28647) and glyceraldehyde 3-phosphate dehydrogenase (GAPDH; CST, catalog #2118S, as loading control) at a 1:1000 dilution. A goat anti-rabbit secondary antibody (Invitrogen, catalog #31460) at a 1:5000 dilution was used for visualization. Western blot data were captured using an imager (ThermoFisher, iBright FL1000) after incubating the membranes in Pierce substrate (ThermoFisher, catalog #32106). The densitometric analysis was calculated using the area under the curve of peak intensity using ImageJ (NIH). Western blot experiments reveal two bands: a stronger band below 53 kDa (~50 kDa) and a weaker band at ~42 kDa. The two bands were only detected when both primary and secondary antibodies were used and no band was detected when excluding either the primary or the secondary antibody

(Extended Data Fig. 7-1*B*). These data further confirmed the specificity of the GPER antibody used for this study.

cDNA synthesis and real-time qPCR (RT-qPCR)

To assess GPER transcripts in cultures, RT-qPCR on the cDNA of RNA samples extracted from hippocampal and cortical cultures at 72 HIC was conducted. The synthesis of cDNA was performed using SuperScript IV VILO Master Mix (Invitrogen, catalog #11766050) following the manufacturer's instructions. The subsequent RT-qPCR was performed on a QuantStudio 5 Real-Time PCR System (ThermoFisher, catalog #A28133) using SYBR Green PCR Master Mix (Applied Biosystems, catalog #4309155). The primers used were: Gper1 forward: CATGCCTACCCCTTGACAGG, reverse: TGGT ATGACTGCCTTGAGCG. For normalization, the housekeeping gene (control) Gapdh was used, with primer sequences: forward: TCAACGGCACAGTCAAGGC, reverse: AGGGATGATGTTCTGGGCTG.

RNA extraction, sequencing, and analysis

To investigate GPER's effect on the neuron transcriptome, neurons were plated at a density of 500–600 cells/mm^2 in 24-well plates (Becton Dickinson) and treated with either 0.1% DMSO (vehicle), E2 (100 nM), or G-1 (100 nM, selective GPER agonist) for 72 h. Subsequently, RNeasy Mini kit (QIAGEN, catalog #74104) was used for RNA extraction according to the manufacturer's instructions. The quality and quantity were measured using NanoDrop (ThermoFisher Scientific).

For RNA sequencing, RNA samples were sent to Novogene (Novogene Corporation Inc.) and the sequencing was performed via Illumina NovaSeq 6000 platform based on the mechanism of SBS (sequencing by synthesis). For significance, a *p*-value cutoff of $p < 0.005$ was used (Benjamini and Hochberg's adjusted *p*-value). Unsupervised hierarchical clustering was performed with R Studio (Rstudio, 2015) using Pearson's correlation distance matrix. Venn diagrams and correlation plots were generated using R Studio. Enrichment analysis was performed using gProfiler (Raudvere et al., 2019). The raw sequencing data generated in this study have been submitted to the NCBI BioProject database under accession number PRJNA759869.

Chemicals

U73122 and U73343 were obtained from Tocris. G-1, G-15, and E2 were developed in Chris Arnatt's lab. All other chemicals and cell culture reagents were obtained from Sigma-Aldrich or ThermoFisher unless stated otherwise.

Statistical analysis

All statistics were conducted in R (Team, 2017) using RStudio (Rstudio, 2015) or GraphPad Prism 9 (GraphPad Software, San Diego, California USA). For transcriptomic data analysis, general code and packages used not stated in specific experiments include checking for packages and installing them, tidyverse (Wickham, 2017), data.table

(Dowle and Srinivasan, 2019), emmeans (Lenth, 2019), multcomp (Hothorn et al., 2019), multicompview (Graves et al., 2015), plyr (Wickham, 2016), dplyr (Wickham et al., 2019), DescTools (Signorell et al., 2019), readxl (Wickham and Bryan, 2019), knitr (Xie, 2019), VennDiagram (Chen and Boutros, 2011), pheatmap (Kolde, 2019), and ggrepel (Slowikowski, 2020). For neurite outgrowth assay, a three-way ANOVA (*F*) test comparing type (cortical vs hippocampal), treatment, and time period followed by Tukey's *post hoc* test was conducted to determine significance. For other experiments, data were statistically analyzed using Student's *t* test or one-way ANOVA, followed by Tukey's *post hoc* test to determine significant differences between treatments and/or cell types. For samples in neurite outgrowth and firing activity studies, which followed non-normal (Gaussian) distribution revealed by the Anderson–Darling, D'Agostino and Pearson, Shapiro–Wilk, and Kolmogorov–Smirnov tests, we also performed nonparametric Kruskal–Wallis (*H*) test followed by Dunn's multiple comparisons *post hoc* test to confirm our conclusions. Values were considered statistically significant at the level of $p < 0.05$. Because of the large datasets in our study and individual points become cluttered and difficult to read in most cases, the data are presented in figures as mean ± SEM. Each experiment was replicated a minimum of three times; the actual $F_{(dfs)}$, *n*, and *p* values were provided in the text or figure legends.

Results

GPER agonists enhance neurite outgrowth in rat E18 hippocampal but not cortical neurons

The development of neuronal processes (neurites, including axons and dendrites) is the essential developmental event that allows for the proper formation of neuron-neuron connections (synapses) during early nervous system development and after nerve injury. We first sought to define the impact of GPER activation on neurite outgrowth of rat E18 hippocampal and cortical neurons. Specifically, hippocampi and cortices were dissected from rat E18 embryo brains and were enzymatically digested followed by gentle mechanical trituration. Neurons were cultured in the absence or presence of GPER agonists and/or antagonists and phase contrast and neurite tracing were performed to evaluate their effects (Fig. 1; Extended Data Fig. 1-1). Based on the selective binding profiles of GPER agonist G-1 and antagonist G-15 (see Materials and Methods) and physiological studies in the field (McCarthy, 2008; de Valdivia et al., 2017; Kumar and Foster, 2020), we initially tested the effects of G-1 alone at 100 nM and G-15 alone at 10 nM on the growth of cultured hippocampal and cortical neurons compared with neurons cultured in vehicle (0.1% DMSO). Our results showed that in hippocampal neurons G-1 alone significantly ($p < 0.01$) increased average neurite outgrowth (μm), while G-15 alone had no effect ($p > 0.05$) compared with vehicle (one-way ANOVA, $F_{(2,638)} = 18.46$, $p < 0.01$; Vehicle: 52.4 ± 3.1, $n = 264$ cells; G-1: 78.1 ± 4.4, $n = 180$ cells; G15: 45.2 ± 4.1, $n = 197$ cells). In contrast to hippocampal neurons, G-1 alone did not affect neurite outgrowth
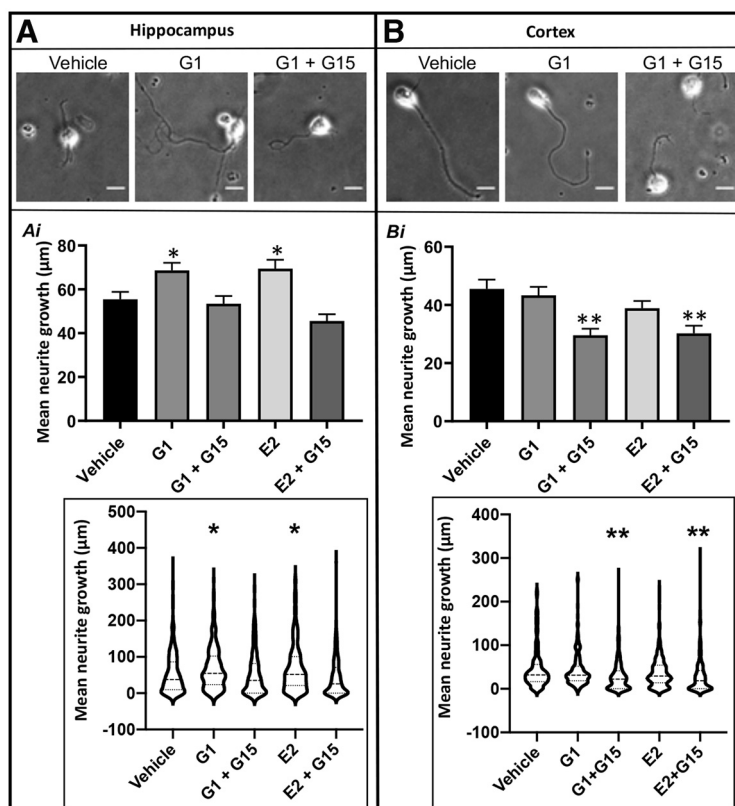
Figure 1. GPER activation increases neurite outgrowth in hippocampal but not cortical neurons. Selected images and results of hippocampal (**A**) and cortical (**B**) neurite outgrowth after 72 HIC. **Ai,** Hippocampal neurons showed an increase in outgrowth compared with vehicle when GPER is activated with the selective agonist G-1 as well as with the nonspecific agonist E2. This effect was inhibited by the GPER-specific antagonist G-15. **Bi,** Cortical neurons showed no significant effect of GPER activation on neurite outgrowth using either G-1 or E2 compared with vehicle control. Cortical neurite outgrowth was inhibited by blocking GPER activation using G-15. Significance was determined using two–way ANOVA followed by Dunnett's test for multiple comparisons (hippocampal, $F_{(7,2527)}$ = 10.73, $p < 0.001$, mean $n = 223$ cells; cortical, $F_{(7,1757)}$ = 8.19, $p < 0.001$, mean $n = 298$ cells). Insets, Violin plot representation of the same datasets as shown in bar graphs. Statistical data of GPER activation/inactivation on hippocampal and cortical neurite outgrowth at all time points from 8 to 96 h are shown in Extended Data Figure 1-1. Data were from three independent experiments; **$p < 0.01$ and *$p < 0.05$, compared with vehicle. Scale bar: 20 μm. Treatments: G-1 (100 nM), E2 (100 nM), G-15 (10 nM).

($p > 0.05$) in cortical neurons, but interestingly, G-15 treatment alone led to significantly reduced growth of cortical neurons compared with their vehicle or G-1 treatment (one-way ANOVA, $F_{(2,245)}$ = 11.6, $p < 0.01$; vehicle: 21.6 ± 2.9, $n = 112$ cells; G-1: 21.3 ± 4.0, $n = 54$ cells; G-15: 4.6 ± 1.5, $n = 82$). These initial experiments revealed intriguing, distinct effects of GPER activation or inactivation on neurite growth in these two different cell types.

To further test the role of GPER activation by agonists on neuronal outgrowth of E18 hippocampal and cortical neurons at different early developing time points, neurons were cultured in vehicle (0.1% DMSO), E2 (100 nM), and G-1 (100 nM), with or without the selective GPER antagonist G-15 (10 nM) for 4 d. Phase-contrast images were taken every day for 4 d, and the ImageJ plugin NeuronJ was employed to measure neurite outgrowth per cell (Schindelin et al., 2012; Imaninezhad et al., 2018; Pemberton et al., 2018; see Materials and Methods). Figure 1 shows the representative images of hippocampal and cortical neurons in vehicle and drug-treated conditions at 72 HIC. Statistical data of GPER activation/inactivation on

hippocampal and cortical neurite outgrowth at all time points from 8–96 h are shown in Extended Data Figure 1-1. Data were collected from cells cultured in three independent experiments with three replications per treatment group at each time point. Overall, a three-way ANOVA comparing type (cortical vs hippocampal), dose/treatment, and time period showed significant differences at each level ($F_{(1,24269)}$ = 346.28, $F_{(7,24269)}$ = 38.78, $F_{(4,24269)}$ = 2710 respectively; all $p < 0.001$) as well as significance between each interaction (type:treatment $F_{(7,24269)}$ = 12.812, type:time $F_{(4,24269)}$ = 151.62, treatment:time $F_{(28,24269)}$ = 14.78, type:treatment: time $F_{(28,24269)}$ = 5.78; all $p < 0.001$). *Post hoc* tests for individual groups showed 8 HIC treatments had no significant difference between any groups compared with vehicle. At each time point after 8 HIC, both hippocampal and cortical neurons showed significant differences between different treatment groups based on one-way ANOVAs (Cortical, 20 HIC $F_{(7,2186)}$ = 11.10, $p < 0.001$; 48 HIC $F_{(7,2077)}$ = 9.52, $p < 0.001$; 72 HIC $F_{(7,1757)}$ = 8.19, $p < 0.001$; 96 HIC $F_{(7,1764)}$ = 24.15, $p < 0.001$: Hippocampal – 20 HIC $F_{(7,3029)}$ = 6.60, $p < 0.001$, 48 HIC $F_{(7,2397)}$ = 6.65,

$p < 0.001$; 72 HIC $F_{(7,2527)} = 10.73$, $p < 0.001$; 96 HIC $F_{(7,1764)} = 14.58$, $p < 0.001$). Specifically, in hippocampal neurons G-1 significantly enhanced neurite outgrowth at 48 and 72 HIC and this effect was attenuated by blocking GPER activation with antagonist G-15, indicating the involvement of GPER activity (72 HIC comparisons vs vehicle; Fig. 1Ai,Bi, insets). E2 also enhanced neurite outgrowth at 72 and 96 HIC which was blocked by G-15, further implicating the involvement of GPER in estrogen action in hippocampal neurons. Interestingly, in cortical neurons, activation of GPER with G-1 or E2 did not significantly increase neurite outgrowth except at 96 HIC. Additionally, inhibition of GPER by G-15 either in the absence or presence of GPER agonists significantly inhibited neurite outgrowth in cortical neurons at 20–96 HIC; in hippocampal neurons this inhibition was only seen at 20 HIC. Because our normality tests with the Anderson–Darling, D'Agostino and Pearson, Shapiro–Wilk, and Kolmogorov–Smirnov tests suggested that the neurite outgrowth data followed a non-normal (Gaussian) distribution pattern, we also performed nonparametric Kruskal–Wallis test followed by post hoc Dunn's multiple comparisons test to determine whether our conclusions could be changed. We found that the significance between different treatment groups compared with vehicle mirrored that of the Tukey test following the parametric ANOVA analyses. For example, the nonparametric Kruskal–Wallis test followed by post hoc Dunn's test also showed that 8 HIC treatments had no significant difference between any groups compared with vehicle in hippocampal neurons ($H_{(4)} = 7.888$, $p = 0.09$), although there was a significant difference in cortical neurons ($H_{(4)} = 42.01$, $p < 0.0001$). Consistently, at each time point after 8 HIC, both hippocampal and cortical neurons showed significant differences between different treatment groups (Cortical, 20 HIC $H_{(4)} = 63.06$, $p < 0.0001$; 48 HIC $H_{(4)} = 104.5$, $p < 0.0001$; 72 HIC $H_{(4)} = 56.6$, $p < 0.0001$; 96 HIC $H_{(4)} = 122.6$, $p < 0.0001$: Hippocampal, 20 HIC $H_{(4)} = 59.19$, $p < 0.0001$, 48 HIC $H_{(4)} = 22.8$, $p < 0.0001$; 72 HIC $H_{(4)} = 57.17$, $p < 0.0001$; 96 HIC $H_{(4)} = 53.44$, $p < 0.0001$). It is important to note here that the nonparametric Kruskal–Wallis test not only agreed well with our initial parametric ANOVA test for detecting significant differences among treatment groups, but also often revealed more robust significance levels (e.g., $p < 0.0001$ vs $p < 0.001$ shown by parametric ANOVA test) in many of our samples, further confirming our conclusions. Together, these data suggest that pharmacological activation or inactivation of GPER induced distinct effects on primary E18 rat hippocampal and cortical neurons. GPER likely plays stimulatory roles in neurite outgrowth of hippocampal neurons, but the effects of GPER activation/inactivation on cortical neurons varied either having no effects or inhibitory effects.

GPER agonists increase neuronal firing activity in hippocampal and cortical neurons with a more potent effect on hippocampal neurons

It is widely accepted that neurons use electrical activity, also referred to as nerve impulses and action potentials, for neuronal signaling. This neuronal activity has been implicated in a myriad of processes including neural development, synaptic transmission, and synaptic plasticity (Spitzer, 2006; Borodinsky and Belgacem, 2016; Luhmann et al., 2016; A.M. Walter et al., 2018; Kato and Wake, 2019). Because of the observed differential neurite outgrowth in hippocampal and cortical neurons in response to GPER activation, we hypothesized that GPER stimulation results in differences in neuronal electrical activity in hippocampal and cortical neurons. To test this hypothesis, noninvasive MEA (multichannel) neurochip interface technology was used to monitor neuronal firing activity from a group of developing neurons before and after exposure to GPER agonists G-1 or E2. Subsequent studies were performed to examine whether neuronal firing activity could be blocked with the GPER antagonist G-15. Overall, our neurochip recording experiments revealed that there was no significant difference in the baseline (before the treatments) frequency of spiking between hippocampal and cortical cultures (unpaired Student's t test, $p = 0.9$; Hippocampal, 982.3 ± 195, $n = 120$ electrodes; Cortical, 914.9 ± 262.4, $n = 480$ electrodes), but the frequency of neuronal activity was significantly increased in both hippocampal and cortical neurons after G1 or E2 treatments, with a more potent effect observed in hippocampal neurons (Fig. 2). The representative trace in Figure 2A shows that hippocampal neurons at rest were spontaneously active (green bars represent program detected spikes). After the application of 100 nM G-1 (Fig. 2B), the firing frequency (spikes/min) was greatly increased. The statistical data for hippocampal cultures (Fig. 2C) show that both G-1 (one-way ANOVA, $F_{(5,474)} = 14.28$, $n = 60$ electrodes for each condition from 3 independent experiments; Tukey's post hoc analysis, $p < 0.001$) and E2 ($p < 0.001$) significantly increased the neuronal firing activity compared with the control, and the increase in neuronal firing was prevented by G-15 pretreatments (G-1 vs G-1 + G-15; $p < 0.001$, E2 vs E2 + G-15; $p < 0.001$). Similar to hippocampal neurons, cortical neurons (Fig. 2D–F) exhibited a significant increase in the frequency of neuronal firing in response to G-1 (one-way ANOVA, $F_{(5,1552)} = 4.66$; Tukey's post hoc analysis, $p < 0.001$, $n = 180$) and E2 ($p < 0.001$, $n = 180$); however, the magnitude of neuronal activity between the hippocampal and cortical neurons differed (4-fold vs 2-fold increase in firing by G-1; Fig. 2C,F). Additionally, in cortical neurons, attenuation of neuronal firing with G-15 was present but not statistically significant ($p = 0.17$, $n = 180$ for G-1 + G-15; $p = 0.88$, $n = 60$ for E2 + G-15). Similar to the neurite outgrowth data, the normality tests show that these samples followed a non-normal distribution. We then performed the Kruskal–Wallis test followed by post hoc Dunn's multiple comparisons test to further confirm our conclusions. Again, the Kruskal–Wallis test mirrored that of parametric ANOVA test results in most comparisons between groups, although a more robust significance level was once again observed in many comparisons. For example, G1 and E2 were found to significantly increase neuronal firing activity in hippocampal (Kruskal–Wallis test, $H_{(5)} = 67.13$, $p < 0.0001$) and cortical ($H_{(5)} = 66.11$, $p < 0.0001$) neurons. Dunn's post hoc analysis showed that in hippocampal neurons, G1
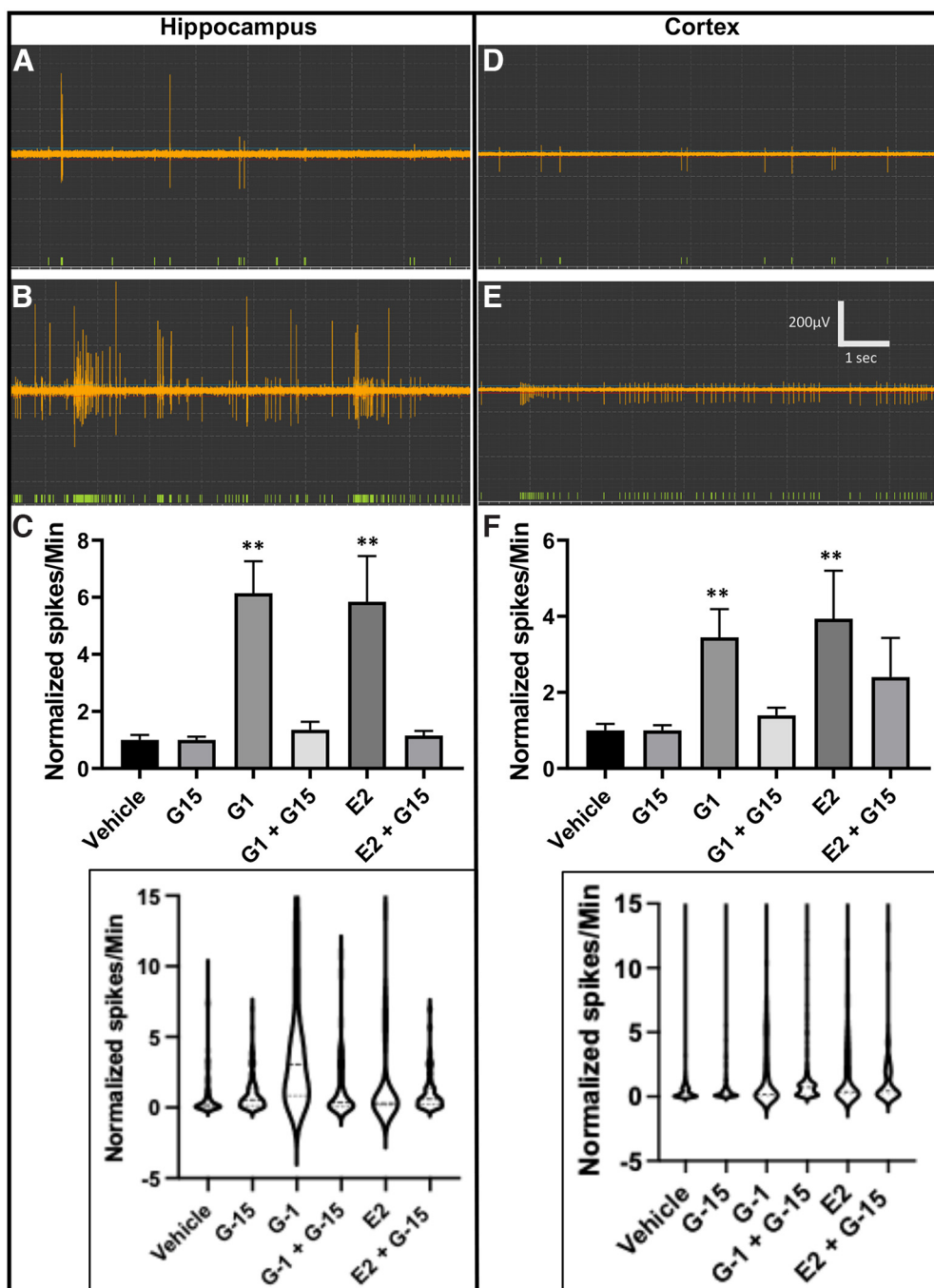
Figure 2. GPER activation increases neuronal firing activity in hippocampal and cortical neurons. Representative readings from hippocampal (*A*, *B*) and cortical (*D*, *E*) neurons show a much lower frequency of spikes (green bars) before the introduction of G-1 (*A*, *D*) compared with the number of spikes after GPER activation using G-1 (*B*, *E*). Statistical data (*C*, *F*) show that both the selective GPER agonist G-1 and nonspecific agonist E2 significantly increase the frequency of neuronal firing activity in hippocampal and cortical neurons cultured for 14 d (values normalized to the response before introduction of the drug as a value of 1). This significant increase in spiking activity from both G-1 and E2 is inhibited by the pretreatment with GPER-specific antagonist G-15 (*C*, *F*). Hippocampus one-way ANOVA, G-1, E2 $F = 14.28$, $p < 0.001$, $n = 60$; cortex one-way ANOVA, G-1, E2 $F = 4.66$, $p < 0.001$, $n = 180$; **$p < 0.01$, compared with vehicle. Treatments: G-1 (100 nM), E2 (100 nM), G-15 (10 nM). Insets, Violin plot representation of the same datasets as shown in bar graphs.

significantly increased firing (vehicle vs G-1, $p < 0.0001$) and the antagonist G15 alone did not affect neuronal activity (vehicle vs G-15, $p > 0.05$), but significantly reduced G-1-induced increase in neuronal activity (G-1 vs G-1+G-15,

$p < 0.0001$). In cortical neurons, G1 significantly increased firing (vehicle vs G-1, $p < 0.0001$), and the antagonist G15 reduced G-1-induced increase in activity, but this reduction did not reach statistical significance level (G-1 vs
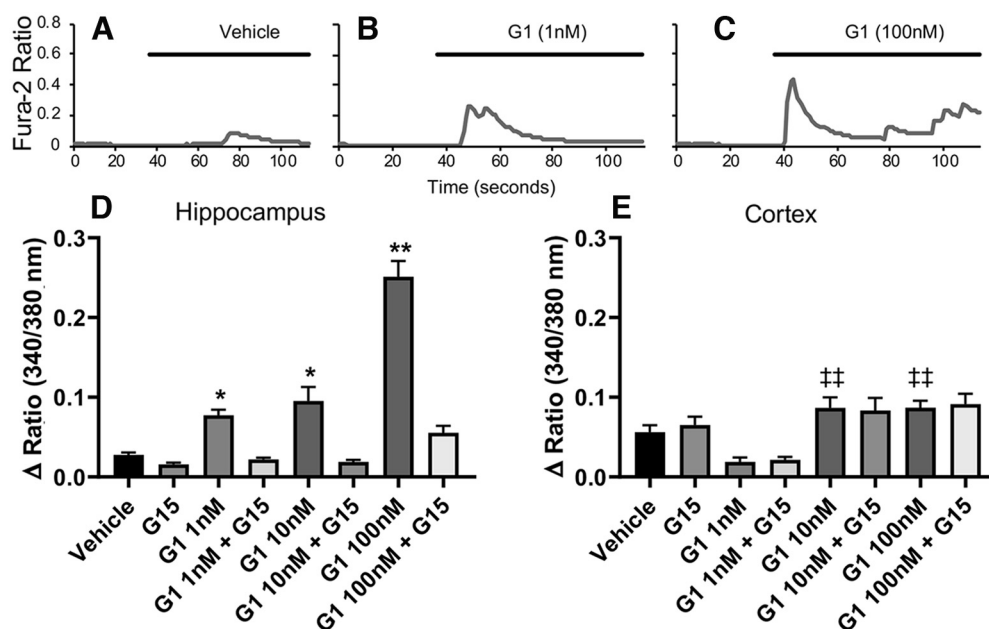
Figure 3. GPER activation increases cytosolic Ca^{2+} in hippocampal but not cortical neurons. Fura-2 ratiometric Ca^{2+} traces of hippocampal neurons (**A–C**) showed a dose-dependent increase in Ca^{2+} response to GPER-selective agonist G-1. Vehicle (**A**) showed little to no Ca^{2+} response while 1 nM G-1 (**B**) showed a significant increase in Ca^{2+} response, and 100 nM G-1 (**C**) showed the greatest increase in Ca^{2+}. **D**, Mean values of peak amplitude of Ca^{2+} increase in hippocampal neurons (one-way ANOVA $F = 80.97$, $n = 92$, Turkey's *post hoc* analysis 1 nM G-1 $p = 0.036$, 10 nM G-1 $p = 0.031$, 100 nM G-1 $p < 0.001$). These effects were blocked by 10 nM G-15. **E**, In cortical neurons, GPER activation lowered levels of Ca^{2+} at 1 nM G-1 while increasing Ca^{2+} at higher concentrations of G-1, although these did not reach significance (G-1 1 nM $p = 0.20$, G-1 10 nM $p = 0.64$, G-1 100 nM $p = 0.45$). These effects were not blocked by G-15; *$p < 0.05$, **$p < 0.01$, compared with vehicle; ‡‡$p < 0.01$, compared with G-1 1 nM.

G-1 + G-15, $p > 0.05$), which is consistent with the parametric ANOVA analysis results. Together, these results demonstrate the pivotal role of GPER in stimulating neuronal activity in hippocampal and cortical neurons although the magnitude of neuronal activity in response to GPER activation/inactivation differs between hippocampal and cortical neurons.

GPER agonists increase Ca^{2+} activity in hippocampal but not cortical neurons

Among ions in flux during neuronal firing is Ca^{2+}, a key second messenger commonly involved in coupling external stimuli and neuronal firing to cytosolic signaling to regulate a variety of neurodevelopmental processes (Rosenberg and Spitzer, 2011; Leclerc et al., 2012). For this reason, we next tested whether Ca^{2+} signaling in response to GPER activation may be altered between hippocampal and cortical neurons. To test this, we conducted fura-2 AM ratiometric Ca^{2+} imaging experiments on both hippocampal and cortical neurons. Our Ca^{2+} imaging data revealed that in hippocampal neurons, GPER activation by G-1 significantly (one-way ANOVA, $F_{(8,1166)} = 80.97$, mean $n = 92$; Tukey's *post hoc* analysis, $p < 0.001$) increased the peak amplitude of Ca^{2+} signals in a dose-dependent manner (1 nM G-1, $p = 0.036$; 10 nM G-1, $p = 0.031$; and 100 nM G-1, $p < 0.001$; Fig. 3A–D) compared with vehicle. The observed increase in Ca^{2+} in response to G-1 and E2 was abolished by pretreatment with the selective GPER antagonist, G-15, for 30 min before treatment. In contrast, cortical neurons did

not exhibit significant change in Ca^{2+} in response to GPER activation as compared with vehicle (Fig. 3E; 1 nM G-1, $p = 0.203$; 10 nM G-1, $p = 0.641$; 100 nM G-1, $p = 0.451$), although there were some significant differences between concentrations of G-1 (one-way ANOVA, $F_{(7,1488)} = 9.46$, mean $n = 182$; Tukey's *post hoc* analysis, $p < 0.001$; G-1 1 nM vs G-1 10 nM $p < 0.001$, vs G-1 100 nM $p < 0.001$). These results show that although GPER activation increased the frequency of neuronal firing activity in cortical neurons, there was no significant change in intracellular Ca^{2+} levels. The absence of Ca^{2+} signaling may contribute to the lack of neurite outgrowth observed in cortical neurons in response to GPER activation. By this same logic, the correlation between electrical activity and Ca^{2+} signaling in response to G-1 and/or E2 in hippocampal neurons may contribute to the GPER-induced neurite outgrowth in these neurons.

GPER agonist-mediated Ca^{2+} rise in hippocampal neurons involves extracellular Ca^{2+} entry via Ca^{2+} channels and internal Ca^{2+} release from phospholipase C (PLC)-inositol trisphosphate (IP_3) Ca^{2+} stores

To gain further insight into the signaling pathway involved in G-1-induced Ca^{2+} rise, the goal of subsequent studies was to understand the source of Ca^{2+} in hippocampal neurons. Intracellular Ca^{2+} mobilization primarily originates from either the influx of extracellular Ca^{2+} or the release of Ca^{2+} from intracellular Ca^{2+} stores.
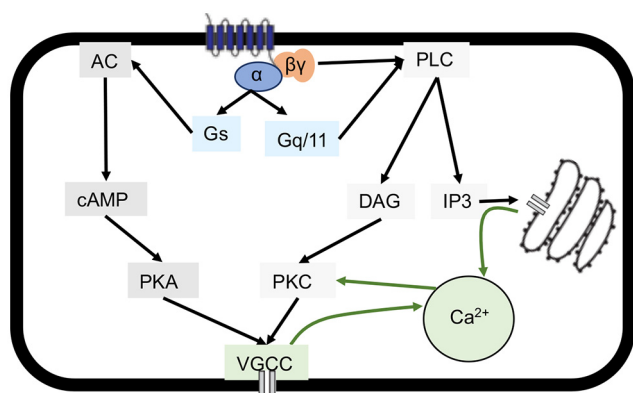
Figure 4. Representative model of common GPCR signaling pathways leading to an increase in cytosolic Ca^{2+}. Different GPCR pathways can converge to an increase in intracellular Ca^{2+} levels. G_s subunit coupling leads to the activation of AC that increases cAMP levels and promotes the activity of PKA. PKA leads to the opening of VGCCs and, therefore, extracellular Ca^{2+} entry via VGCCs. $G_{q/11}$ subunit coupling leads to the activation of PLC which catalyzes the production of DAG and IP_3. IP_3 can then bind to IP_3 receptor-gated Ca^{2+} channels present on the endoplasmic reticulum, leading to Ca^{2+} release from intracellular stores. The subsequent rise in intracellular Ca^{2+}, together with DAG, activates PKC which causes the opening of VGCCs. The $\beta\gamma$ dimer of G-proteins has also been shown to activate PLC or directly regulate VGCCs and lead to an increase in cytosolic Ca^{2+}.

Canonical GPCR Ca^{2+} signaling is illustrated by a schematic drawing in Figure 4. The canonical method of GPCR Ca^{2+} mobilization occurs through the coupling to the $G_{q/11}$-PLC-IP_3-Ca^{2+} channels on the endoplasmic reticulum that are gated by IP_3 receptor. An alternative signaling pathway for Ca^{2+} mobilization can occur through coupling to G_s-adenylate cyclase (AC)-cAMP-protein kinase A (PKA)-voltage-gated Ca^{2+} channels (VGCCs). In addition to these pathways, PLC-induced production of DAG can subsequently activate protein kinase C (PKC), which in turn leads to the opening of VGCC and an increase in intracellular Ca^{2+}. Lastly, the $\beta\gamma$ dimer of G-proteins has also been shown to activate PLC or directly modulate VGCCs for Ca^{2+} mobilization (De Waard et al., 1997; Uezono et al., 2004; Smrcka, 2008; Proft and Weiss, 2015). The potential involvement of store-operated Ca^{2+} channels (SOCs) which is activated by the depletion of Ca^{2+} from the endoplasmic reticulum (Prakriya and Lewis, 2015) is not included in the schematic drawing. Because GPER has been shown to increase the level of cAMP in hippocampal neurons (Evans et al., 2016) and both cAMP and the downstream effector PKA have been shown to regulate Ca^{2+} signaling (Taylor, 2017), we first sought to determine the involvement of the G_s/cAMP/PKA pathway in G-1-induced Ca^{2+} rise in hippocampal neurons using a selective inhibitor of adenylyl cyclase [AC; 2′,3′ dideoxyadenosine (DDA), 10 μM; Leavitt et al., 1987; Amendola et al., 2012] to inhibit cAMP production. Specifically, hippocampal neurons were pretreated with vehicle or DDA alone for at least 30 min before exposure to G-1. Figure 5 shows the δ (Δ) level of increase in mean

peak amplitude or frequency of Ca^{2+} spikes by G-1 over basal Ca^{2+} level in vehicle or DDA alone (data not shown). The results (Fig. 5) showed that 100 nM of G-1 (one-way ANOVA, $F_{(4,473)}$ = 22.38; Tukey's *post hoc* analysis, $p < 0.001$, $n = 131$ cells) significantly increased the peak amplitude of Ca^{2+} spikes compared with vehicle and that pretreatment with DDA failed to prevent the increase in Ca^{2+} amplitude because of G-1 ($p < 0.001$, $n = 138$ cells) compared with DDA alone ($n = 90$ cells). Moreover, both G-1 and G-1 plus DDA significantly increased the frequency of Ca^{2+} spikes (G-1 alone, $p < 0.05$, $n = 40$ neurons; G-1 with DDA, $p < 0.05$, $n = 43$) compared with vehicle ($n = 72$). These data were from four replications with three trials. These data indicate that the G_s/cAMP/PKA may not be directly involved in GPER-mediated regulation of Ca^{2+} in hippocampal neurons.

We then examined whether G-1-induced intracellular Ca^{2+} involves the activation of PLC-IP_3 pathway in hippocampal neurons. To this end, neurons were pretreated with a selective PLC inhibitor, U73122 (10 μM), and its inactive form, U73343 (10 μM; Jin et al., 1994; Takenouchi et al., 2005) for at least 30 min before exposure to G-1. Our data showed that G-1-induced Ca^{2+} increase was abolished with the PLC inhibitor U73122 (one-way ANOVA, $F_{(5,271)}$ = 22.39, Tukey *post hoc* analysis; $p = 0.999$ vs vehicle control; $p < 0.001$ vs G-1 alone), while the Ca^{2+} increase remained using the inactive analog U73343 ($p < 0.001$ vs vehicle; $p = 0.996$ vs G-1 alone; Fig. 6A–D,G). We also found that chelerythrine chloride, a selective inhibitor of PKC, the downstream effector of PLC-diacylglycerol (DAG)-Ca^{2+}, did not affect the ability of G-1 to increase Ca^{2+} in hippocampal neurons. Specifically, the change in Ca^{2+} ratio in G-1 alone was 0.46 ± 0.04 ($n = 54$) and in G-1 + chelerythrine chloride was 0.48 ± 0.02 (one-way ANOVA, $F_{(4,473)}$ = 22.38, Tukey's *post hoc* analysis; $p > 0.05$ vs G-1 alone, $n = 58$; data not shown). These data indicate that PKC is not responsible for independently activating Ca^{2+} channels. Based on the findings with the PLC inhibitor, U73122, and the PKC inhibitor, chelerythrine chloride, it appears that at least some of the Ca^{2+} mobilization in response to GPER activation occurs through the PLC-IP_3 signaling cascade.

Pertaining to GPER, evidence also suggests that the L-type Ca^{2+} channel Cav1.3 is responsible for estrogen-stimulated Ca^{2+} influx in endometrial cancer and vascular smooth muscle cells (Hao et al., 2015; Ji et al., 2016). Therefore, we next also examined the involvement of extracellular Ca^{2+} entry in response to GPER activation in hippocampal neurons. To do this, we used either a Ca^{2+}-free buffer (Fig. 6E) or added a commonly used nonselective VGCC blocker, cadmium chloride ($CdCl_2$; Fig. 6F; Dascal et al., 1986; Tredway et al., 1999; Chin et al., 2003; Martínez Damonte et al., 2018; Lee et al., 2022) to block extracellular Ca^{2+} entry via VGCCs. We found that in assays with Ca^{2+} supplemented buffer, G-1 increased the intracellular Ca^{2+} level in hippocampal neurons compared with vehicle (Fig. 6E–G), and this rise in Ca^{2+} mobilization in response to GPER activation by G-1 was significantly attenuated in a Ca^{2+}-free buffer or with $CdCl_2$ (100 μM;
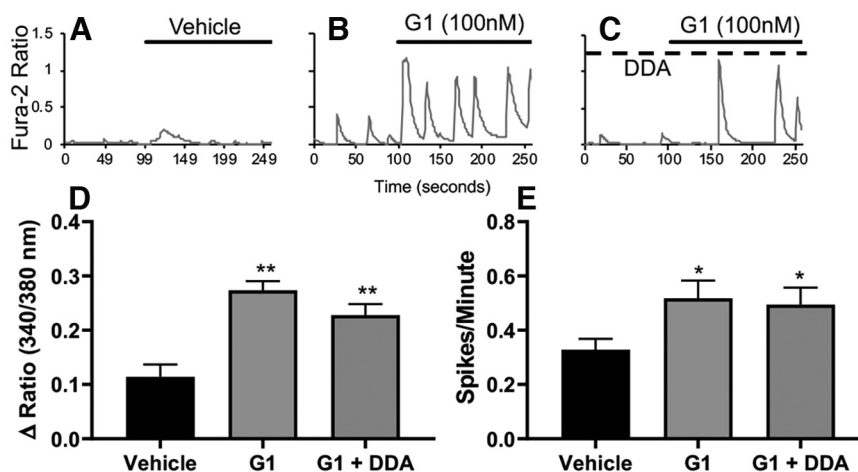
Figure 5. GPER- induced Ca^{2+} rise is not dependent on cAMP production. ***A–C***, Representative traces of fura-2 ratiometric Ca^{2+} imaging for vehicle (***A***), G1 alone (***B***), and G1 with selective inhibitor of AC DDA (10 μM; ***C***). Statistical data demonstrate that G-1 still significantly increased both the mean values of peak amplitude of Ca^{2+} increase (***D***) and the mean frequency of Ca^{2+} spiking activity (***E***) when cAMP production is inhibited by DDA (G-1 $p < 0.001$, $n = 131$, DDA + G-1 $p < 0.001$, $n = 138$, vehicle $n = 90$); *$p < 0.05$ and **$p < 0.01$, compared with vehicle.

one-way ANOVA, $F_{(5,271)} = 22.39$, Tukey's *post hoc* analysis; $p < 0.05$ vs G-1 for both). These data indicate that G-1-induced Ca^{2+} rise involves extracellular Ca^{2+} entry likely via VGCCs. It is important to note that Ca^{2+} rise in response to G-1 in the absence of external Ca^{2+} or with $CdCl_2$ still exhibited significant Ca^{2+} rise compared with vehicle ($p < 0.001$ vs vehicle control for both scenarios), further indicating that internal Ca^{2+} store release also contributes significantly to GPER-mediated Ca^{2+} rise in hippocampal neurons.

Together, our Ca^{2+} imaging experiments showed that G-1 increases cytosolic Ca^{2+} in rat hippocampal, but not cortical, neurons. This rise in hippocampal intracellular Ca^{2+} involves both internal Ca^{2+} release mediated by the PLC-IP$_3$ pathway and external Ca^{2+} entry potentially via VGCCs. The interplay of Ca^{2+} from both sources is essential for the maintenance of spontaneous Ca^{2+} spiking activity (oscillations) and the G-1-mediated increase in intracellular Ca^{2+} in hippocampal neurons. The different effectiveness of GPER on Ca^{2+} signaling in rat E18 hippocampal versus cortical neurons may partially contribute to its distinct effects on neurite outgrowth in cultured hippocampal and cortical neurons. Next, we sought to determine the molecular mechanisms that might contribute to the distinct effects of GPER-medicated neural outgrowth of hippocampal and cortical neurons.

GPER expression in E18 hippocampal and cortical primary cultures and tissues

We hypothesized that a richer expression of GPER in hippocampal neurons may account for the stronger effects of GPER in hippocampal neuronal growth and activity. We first determined whether differential expression or distribution of GPER occurred in cultured rat E18 hippocampal and cortical neurons. Hippocampal and cortical neurons were cultured, fixed at 72 HIC, and fluorescently stained with antibodies against GPER (red; Invitrogen,

catalog #PA5-28 647) and MAP2 (neuronal dendritic marker, green; Invitrogen, catalog #13-1500) with DAPI (blue) labeling nuclei. The results show that GPER is abundantly expressed in both hippocampal and cortical neurons. While in both cell types GPER expression is strong in the cell bodies (indicated by arrowheads), it is also weakly expressed in the neurites (Fig. 7A, arrows). Subcellularly, GPER is largely located in the cytosol as well as in the nuclear area of both hippocampal and cortical neurons. Overall, there is no apparent difference in GPER's localization at distinct neuronal compartments (soma vs neurite) or subcellular structures in hippocampal and cortical neurons. Next, we tested whether the expression level of GPER differs between hippocampal and cortical neurons by measuring GPER mRNA via RT-qPCR and GPER protein expression via Western blotting. For qPCR, hippocampal and cortical neurons were cultured for 72 h and RNA was extracted for subsequent measurement of GPER transcripts. To our surprise, qPCR data (Fig. 7B) showed that GPER transcripts are significantly more abundant in cortical cultures than hippocampal cultures ($p < 0.05$, unpaired Student's t test, $n = 5$ replications). This result contradicts our original postulation that a more robust physiological response to G-1 in hippocampal compared with cortical cultures corresponds to a greater GPER mRNA expression. We then wondered whether GPER protein level has higher expression in hippocampal than in cortical cells. Unfortunately, the small amount of proteins extracted from primary cultures did not yield clear and reliable bands of GPER proteins when assayed with Western blotting. We then performed a Western blotting using *ex vivo* tissues of rat E18 hippocampus and cortex. Specifically, bilateral hippocampus and cortex from individual E18 embryos were harvested, sonicated, and suspended in lysis buffer in preparation for Western blotting with antibodies to GPER (Invitrogen, catalog #PA5-28 647) and GAPDH (CST, catalog #2118S, as
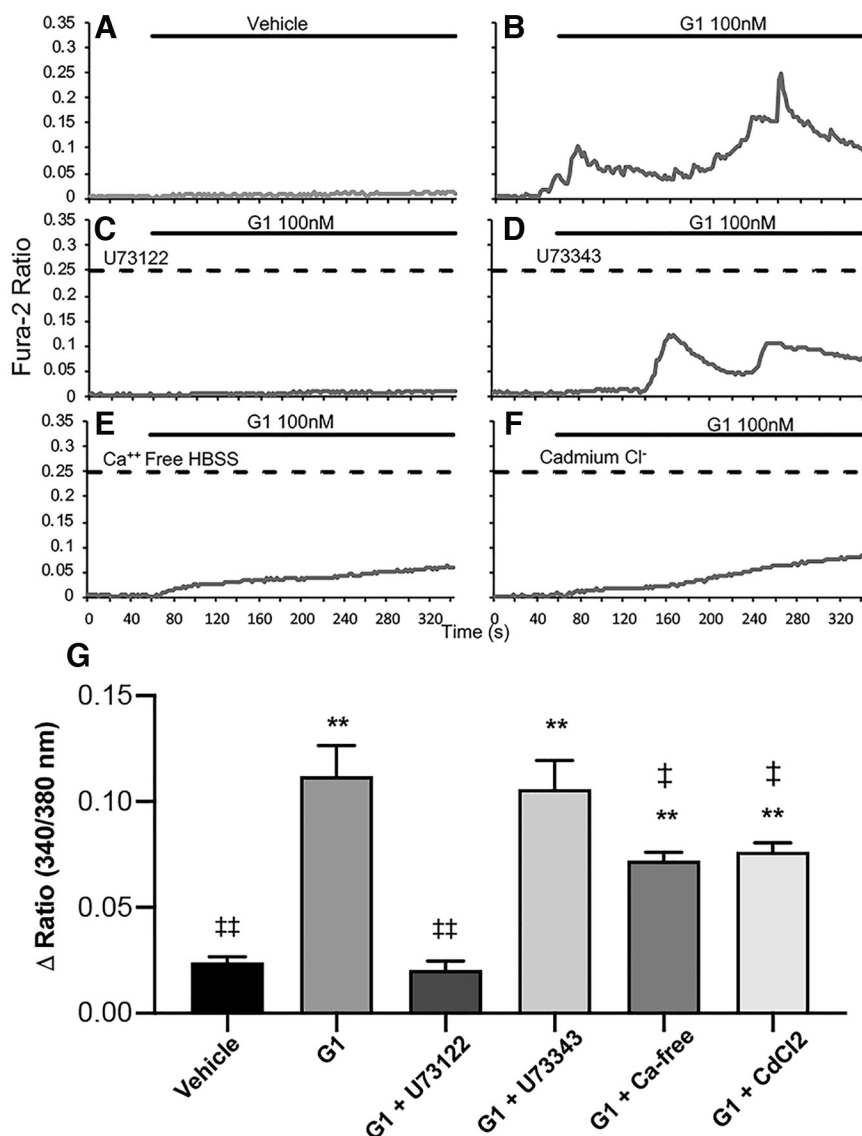
Figure 6. GPER-induced Ca^{2+} rise in hippocampal neurons involves both extracellular Ca^{2+} entry via VGCCs and PLC-mediated internal Ca^{2+} store release. **A–F,** Representative traces of ratiometric Ca^{2+} imaging in vehicle (**A**), G-1 alone (**B**), G-1 plus PLC inhibitor (U73122, 10 μM; **C**), G-1 plus the inactive analog of the PLC inhibitor (U73343, 10 μM; **D**), G-1 in Ca^{2+}-free buffer (**E**), and G-1 plus 100 μM cadmium Cl- (CdCl$_2$), a nonspecific blocker of VGCCs (**F**). **G,** Statistical data show that GPER-induced increase in intracellular Ca^{2+} is blocked fully by inhibition of IP_3 production (U73122 $p = 0.999$ vs vehicle, $p < 0.01$ vs G-1), but only partially, yet significantly, inhibited by removal of external Ca^{2+} ions (Ca^{2+}-free; $p < 0.05$ vs G-1) or by blocking of Ca^{2+} entry with CdCl$_2$ ($p < 0.05$ vs G-1); **$p < 0.01$ versus vehicle, ‡$p < 0.05$ versus G-1, ‡‡$p < 0.01$ versus G-1.

loading control). Western blotting detected two bands in both hippocampal and cortical tissues (Fig. 7C): one stronger band at ~50 kDa and one weaker band at ~42 kDa. The lower GPER mass species such as ~42 kDa and higher band protein species were reported previously and were found to be caused by GPER N-glycosylation or nonglycosylation (de Valdivia et al., 2017, 2019). Interestingly, our data showed that the normalized ratio of GPER:GAPDH (AU) was significantly higher in the cortex (Cx) than hippocampus (Hp) for the 50 kDa; GPER at 42 kDa showed a higher expression in the cortex, but the level of difference was not statistically significant ($p > 0.05$, unpaired Student's t

test, $n = 10$ animals from three preparations). Overall, these experiments indicate that there is no apparent difference in GPER localization in hippocampal and cortical neurons, yet GPER mRNA level measured by qPCR in cortical cultures is significantly higher than in hippocampal cultures. Similarly, GPER protein level (specifically the ~50 kDa) appears to be more abundant in E18 rat cortex than in the hippocampus. Taken together, these data did not support our hypothesis that the robust GPER stimulatory action in hippocampal neurite outgrowth, firing, and Ca^{2+} rise may depend on GPER being more heavily expressed in hippocampal neurons. These data instead indicate that the difference in physiological
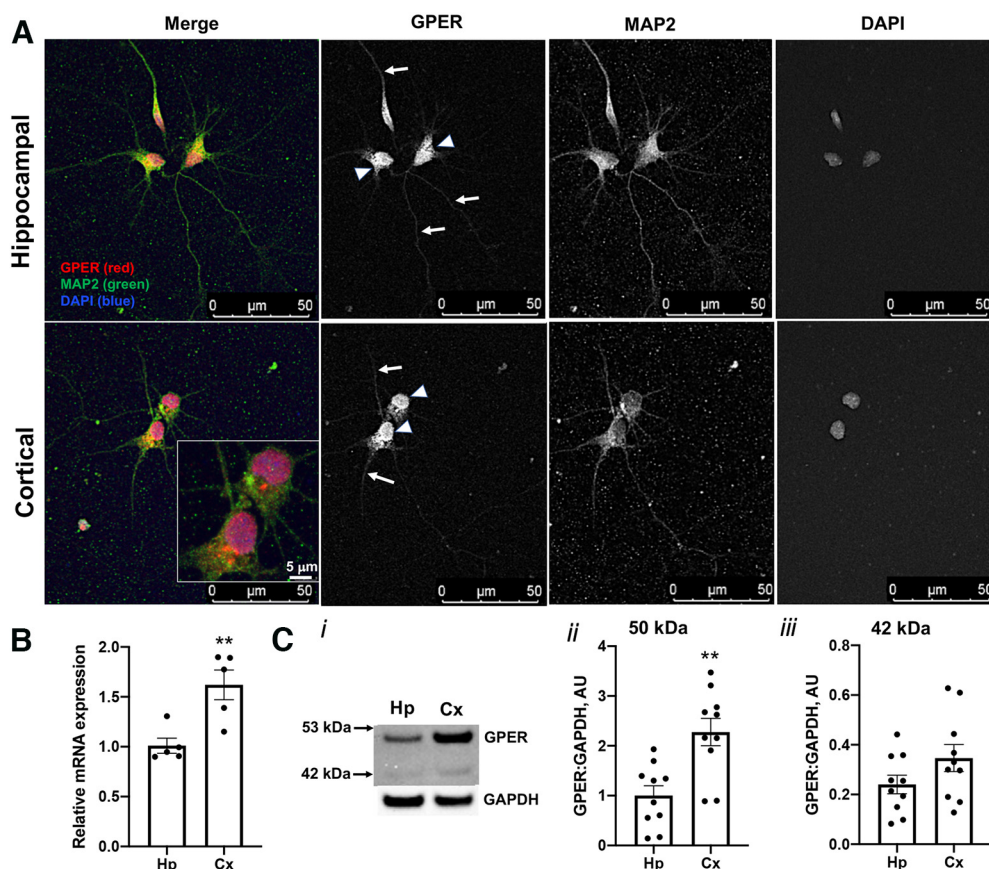
Figure 7. Studies of GPER expression in hippocampal and cortical cultures and tissues. GPER expression and localization in cultured hippocampal and cortical neurons 72 HIC were measured using immunofluorescent and confocal microscopy techniques. **A**, Representative fluorescence images showing the localization of GPER (red) in cell bodies (arrowheads) and neurites (arrows). Cell nuclei are labeled with DAPI (blue) and neurites are labeled with MAP2 (green). **B**, RT-qPCR measurement of the relative GPER mRNA level in samples derived from hippocampal and cortical culture at 72 HIC shows a significantly (unpaired Student's t test, $p < 0.01$, $n = 5$ replicates) higher GPER mRNA level in cortical than hippocampal cultures. **C**, Western blot measurements of GPER protein expression in *ex vivo* hippocampal and cortical tissues from individual E18 rat brains ($n = 10$) reveals two protein species with mass sizes of ~50 and 42 kDa (***i***). Statistical analysis shows that expression of GPER ~50 kDa is significantly higher in cortical than in hippocampal tissues (***ii***), while GPER ~42 kDa is slightly, but not significantly, higher in cortical than in hippocampal tissues (***iii***). Unpaired Student's t test; **$p < 0.01$. The specificity of the GPER antibody used for this study was validated by immunocytochemistry and Western blotting. The validation results are shown in Extended Data Figure 7-1.

response by cell type may be because of other cellular mechanisms such as heterotrimeric G-protein association, cellular signaling, and specific molecular effector coupling. For this purpose, we performed RNA sequencing to explore the potential genes and pathways that might contribute to the distinct effects of GPER-mediated neuronal outgrowth of hippocampal and cortical neurons.

RNA sequencing data revealed different transcriptomic effects of GPER agonists on hippocampal and cortical neurons

We conducted RNA sequencing experiments on G-1, E2, and vehicle-treated hippocampal and cortical cultures. Specifically, isolated rat E18 hippocampal and cortical neurons were cultured in vehicle (0.1% DMSO), G-1 (100 nM), or E2 (100 nM). After 72 HIC, RNA was extracted and sent to Novogene for RNA sequencing using the Illumina NovaSeq 6000 platform. For each group, three

biological replicates were used and gene expression levels were normalized as fragments per kilobase of transcript sequence per million base pairs (FPKM). The observed transcriptomic changes were stronger in hippocampal compared with cortical cultures, but in both tissue cultures, E2 treatment yielded greater transcriptomic changes compared with G-1 treatment, indicating a broader, nonselective profile for E2. More specifically, in hippocampal cultures, the treatment of E2 yielded 1200 significantly differentially expressed (DE) genes compared with vehicle, while the specific GPER agonist G-1 had 159 significantly DE genes. In cultured cortical neurons, E2 led to 157 significantly DE genes and G-1 led to eight significantly DE genes. Interestingly, unsupervised hierarchical clustering using the log2(FPKM + 1) values showed a clear separation of transcriptomes between hippocampal and cortical cultures (Fig. 8A). The hierarchical clustering also revealed that G-1 and E2 treatment have a different outcome on the transcriptome in the two tissue cultures:
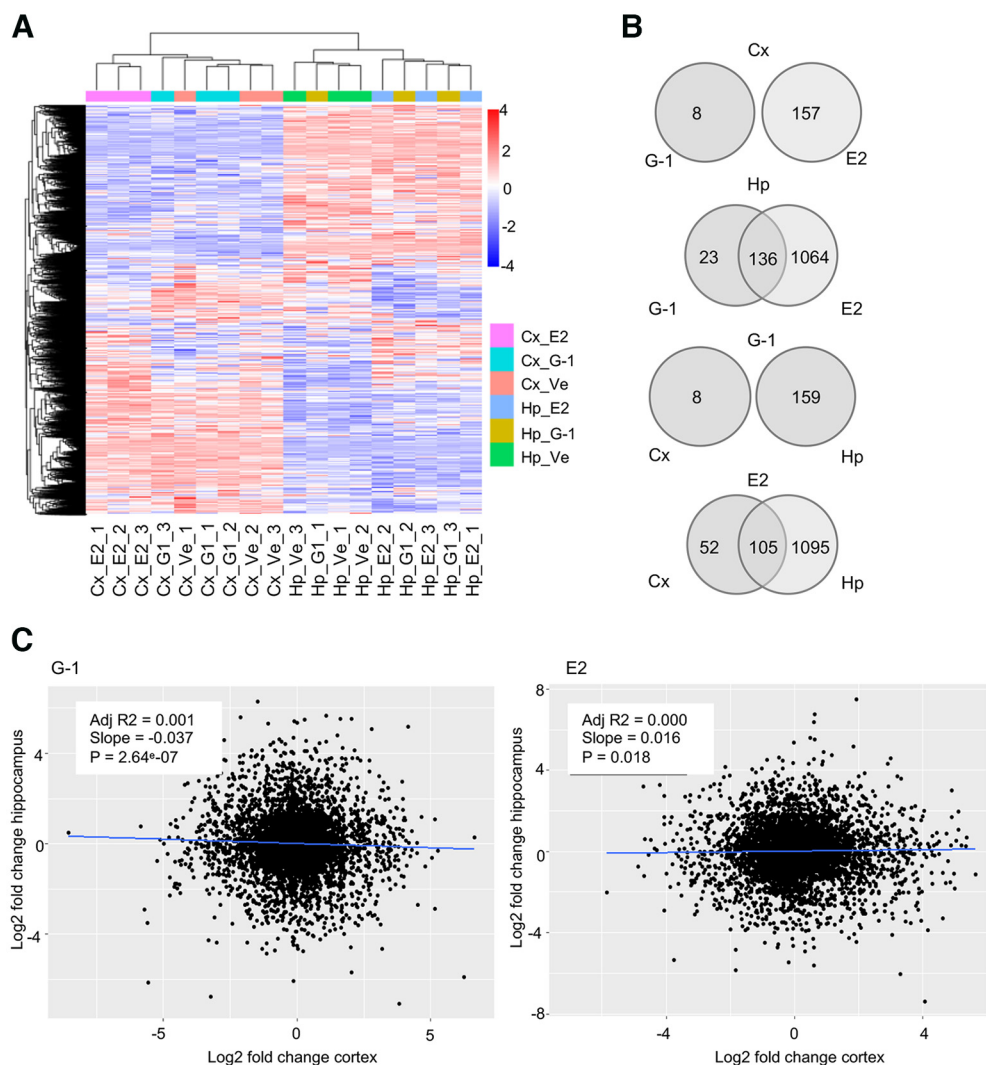
Figure 8. RNA sequencing data show different transcriptome changes in hippocampal versus cortical cultures after G-1 or E2 treatment. RNA sequencing was performed on hippocampal or cortical cultures treated with vehicle, G-1 (100 nM), or E2 (100 nM) for 72 h: a total of 18,749 genes were identified (n = 3 for each group). ***A***, Heatmap showing the differential expression of genes in cortical (Cx) compared with hippocampal (Hp) cultures. The hierarchical clustering of the log2(fpkm + 1) values shows the separation of transcriptome between cortical and hippocampal cultures. Furthermore, the clustering reveals that in cortical cultures, G-1 treatment has little to no effect, clustering with vehicle, while in hippocampal cultures, both G-1 and E2 treatment are separated from vehicle. ***B***, Venn diagrams showing the overlap of significantly regulated genes among different primary cultures or treatments. In cortical samples, eight genes were significantly regulated by G-1 and 157 by E2 compared with the vehicle (p < 0.005, FDR adjusted p-value) with no overlap between the treatments, indicating that in cortical cultures G-1 and E2 significantly regulate two distinct sets of genes. In hippocampal samples, 159 genes were significantly regulated by G-1 and 1200 by E2 compared with the vehicle (p < 0.005, FDR adjusted p-value), and ~85% (136 out of 159) of genes significantly regulated by G1 are also significantly regulated by E2 treatment. Moreover, there is no overlap between cortical and hippocampal cultures treated with G-1, while E2 significantly regulates 105 genes in both cultures. ***C***, Correlation plots show no correlation among cortical and hippocampal genes' log2 fold change compared with vehicle after treatment with either G-1 or E2.

in hippocampal primary cultures, both G-1 and E2-treated samples clustered separately from the vehicle control, while in cortical primary cultures, E2, but not G-1, treated samples clustered separately from the vehicle control. Moreover, Venn diagrams showed that in hippocampal cultures ~85% of DE genes (136 out of 159 genes) were commonly regulated by G-1 or E2, while there was no overlap in the DE genes after G-1 or E2 treatment in cortical cultures (Fig. 8B). Next, we performed correlation

plots, using the log2 fold change values, compared with vehicle controls, of E2 or G-1 in both cortical and hippocampal cultures (Fig. 8C). The log2 fold change values were used to correct for any difference in gene expression because of the different tissue cultures. The correlation plots further confirmed that both G-1 and E2 treatments yield very different transcriptome changes in the two different tissue cultures. Together, these data indicate that GPER action may affect the transcriptome profiles

differently in hippocampal and cortical neurons, with a more robust effect on hippocampal than cortical neurons.

In addition, the Gene Ontology (GO) analysis, performed using gProfiler (Raudvere et al., 2019), revealed differences in enriched pathways in hippocampal and cortical cultures. Specifically, results from hippocampal cultures show that both G-1 and E2 significantly regulate pathways (indicated by asterisks) related to "nervous system development" (GO:BP G-1 adj. $p = 1.2e-06$, E2 adj. $p = 1.47e-16$) that includes the adhesion molecules genes *Nrcam* and *Adgrb2*, "intracellular anatomic structure" (GO:BP G-1 adj. $p = 0.00$, E2 adj. $p = 1.55e-54$) that includes the neurofilament protein gene *Nefm*, and "cytoskeletal protein binding" (GO:BP G-1 adj. $p = 4.01e-05$, E2 adj. $p = 4.01e-05$) that includes the actin-binding protein genes *Cfl1*, *Pfn1*, and *Fscn1*. In addition, E2 also showed significant enrichment for "organelle" (GO:CC adj. $p = 2.32e-43$) that includes synaptic vesicle genes such as *Syt4*, *Stxbp1*, and *Snap25* and "protein binding" (GO:MF adj. $p = 9.74e-19$) that includes the semaphoring genes *Sema3a*, *Sema5a*, and *Sema4c*. The G-1 group also showed significant enrichment for "axon guidance" (KEGG adj. $p = 0.023$) that includes genes involved in axon and dendrite growth like *Dpysl5*, *Dpysl3*, and *Gap43*, and "synapse" (GO:CC adj. $p = 5.77e-06$) that includes genes involved in signaling like *Calm2* and adhesion molecules like *Nrcam* (Fig. 9A, top five terms ranked by adjusted p-value). In cortical cultures, E2 treatment showed a significant enrichment for "synaptic signaling" (GO:BP synaptic signaling adj. p-value = 0.018; chemical synaptic transmission adj. p-value = 0.047) including genes like *Calm2* and *Syp*, "ribosome" (GO:CC adj. $p = 9.12e-06$) including ribosomal genes like *rps2*, *rps7*, *rps23*, *rpl9*, *rpl13*, and *rpl32*, and "NADH dehydrogenase activity" (GO:MF NADH dehydrogenase activity adj. $p = 0.0004$) including mitochondrial genes like *Mt-nd1*, *Mt-nd2*, *Mt-nd3*, *Mt-nd5*, and *Mt-nd6* (Fig. 9B, top five terms ranked by adjusted p-value). Interestingly, there is only one significant enrichment revealed for G-1 significantly regulated genes in cortical cultures (KEGG: sulfur relay system adj. $p = 0.036$) that includes only the cysteine desulfurase, mitochondrial-like gene LOC100911034. The slight effect of G-1 in cortical cultures is further shown by volcano plots (Fig. 9C). Lastly, our analysis of DE genes in hippocampal cultures also shows the significant regulation of GPCR signaling genes (*Rangap1* and *Gpsm1*) and protein kinase signaling genes (*Camk2b* and *Akt1*) in hippocampal but not cortical cultures. The list of the above-mentioned and other top DE genes in both cultures by either G1 or E2 was provided in Extended Data Figures 9-1 (hippocampal) and 9-2 (cortical).

Discussion

This study sought to determine the role of GPER in the early neurodevelopment of rat E18 hippocampal and cortical neurons. Our experiments show that estrogen/GPER signaling exhibits strong neurotrophic effects through increased neurite growth in hippocampal, but not cortical, neurons. Activation of GPER also increases action potential firing and Ca^{2+} signaling more robust in hippocampal than in cortical neurons. RNA sequencing data further revealed significantly distinct DE genes and enriched pathways that are regulated by GPER activity in hippocampal versus cortical neuronal cultures. Specifically, this study identified potential molecular targets such as genes involved in axonal/dendritic growth, cytoskeletal binding, adhesion molecules, and G-protein/protein kinase signaling that may contribute to GPER's neurotrophic effects in hippocampal neurons during early neuronal development. These results are important for our fundamental knowledge of estrogen functions via GPER signaling in different types of neurons during early nervous system development.

Identification of GPER as a neurotrophic promotor for neurite outgrowth of rat E18 hippocampal, but not cortical, neurons

GPER has higher levels of expression in the brain relative to classical ERs (Hutson et al., 2019) and alteration of GPER or its signaling pathways has been found in patients with autism spectrum disorder and schizophrenia (Altun et al., 2017), suggesting that GPER may play a crucial role in the pathophysiology of these neuropsychiatric disorders. Research into autism and schizophrenia has looked at alterations at the neurodevelopmental level; however, there is limited research into understanding the neurodevelopmental impacts of targeting GPER. Here, we found that GPER activation increased neurite outgrowth, which is consistent with previous studies showing that E2 increased neuritogenesis in primary mouse E17 hippocampal neurons via GPER activation (Ruiz-Palmero et al., 2011, 2013). Earlier studies have demonstrated that E2 exposure increases the number and length of neuritic filopodia in primary rat E18 hippocampal neurons within minutes of exposure, although it is not clear whether this action is mediated by GPER because of the lack of knowledge of this receptor at that time (Brinton, 1993). Nevertheless, these studies indicate a neurotrophic role of GPER in promoting early development in hippocampal neurons.

In cortical neurons, our and other studies have shown that the effect of estrogen or GPER activation/inactivation appears more variable in magnitude and direction in terms of neurite outgrowth. Brinton et al. (1997) demonstrated that E2 differently regulates cortical neural outgrowth with a significant enhancement in parietal and occipital neurons, no significance in frontal neurons, and an inhibitory effect on temporal neurons. Furthermore, these results were not inhibited by the nuclear ER antagonist ICI 182780, suggesting that there may be a GPER-related mechanism. Consistently, our rat E18 mixed cortical neurons revealed highly variable effects in terms of the magnitude (potency) and direction (stimulation vs inhibition) of GPER agonists such as E2 and G-1.

Interestingly, our results also showed the GPER antagonist G-15 alone significantly inhibited cortical, but not hippocampal, basal outgrowth. It is not known whether the inhibitory effect of G-15 is because of nonspecific binding to nuclear ERs, which are important for maintaining the basal growth of cortical neurons. However, the 10 nM G-15 we used is far below the concentration (10 μM) for nonspecific binding to ERs (Dennis et al., 2011). This then
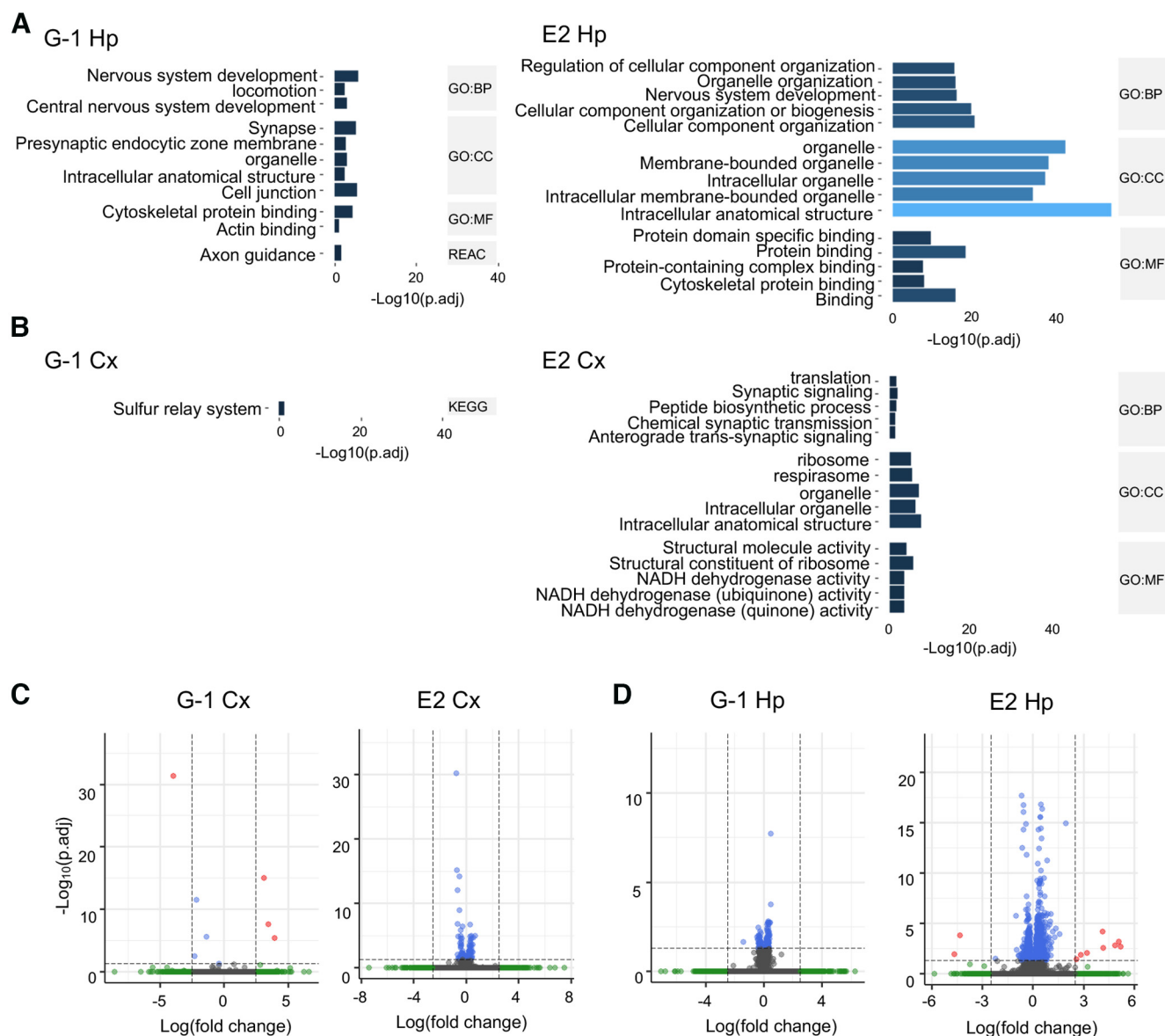
Figure 9. Pathway enrichment and correlation analysis show that GPER activation leads to specific changes in gene expression in hippocampal versus cortical neurons. ***A***, ***B***, Pathway enrichment analysis shows different enrichment of hippocampal (Hp) or cortical (Cx) samples after G-1 (100 nM) and E2 (100 nM) treatment. Only the top five significant enrichment terms ranked by p-value are shown (-Log10 adj. $p > 1.3$). ***A***, In hippocampal cultures, both G-1 and E2 are enriched for genes involved in nervous system development (GO:BP G-1, adj. $p = 1.2e-06$; E2, adj. $p = 1.47e-16$). Moreover, G-1 treatment shows enrichment for synapse (GO:CC, adj. $p = 5.77e-06$), cytoskeletal protein binding (GO:MF, adj. $p = 4.01e-05$) and axon guidance (KEGG, adj. $p = 0.023$). E2 treatment shows enrichment for organelle (GO:CC, adj. $p = 2.32e-43$) and protein binding (GO:MF, adj. $p = 9.74e-19$). ***B***, Transcriptome data from cortical cultures treated with G-1 show almost no enrichment, with only one significant GO term (KEGG: sulfur relay system). E2 treatment shows significant enrichment for synaptic signaling (GO:BP synaptic signaling, adj. $p = 0.018$; chemical synaptic transmission, adj. $p = 0.047$), ribosome (GO:CC, adj. $p = 9.12e-06$), and NADH dehydrogenase activity (GO:MF NADH dehydrogenase activity, adj. $p = 0.0004$). ***C***, ***D***, Volcano plots showing differentially expressed genes. The dashed line shows the $p < 0.05$ cutoff (FDR adjusted p-value). Genes are represented as dots color-coded in gray (not significant, below log2 fold change threshold), green (above log2 fold change threshold > |2.5|), blue (significant, FRD adj. $p < 0.05$), and red (significant and above the log2 fold change threshold). The top DE genes in hippocampal and cortical cultures regulated by either G1 or E2 are provided in Extended Data Figures 9-1 (hippocampal) and 9-2 (cortical).

poses other possibilities that may explain the observed differences in hippocampal and cortical neurons in response to G-15. For example, GPER displays greater constitutive activity in cortical neurons than in hippocampal neurons, which may be related to either an increase in

expression of the transducer associated with receptor signaling or through a greater degree of endogenous synthesis of estrogen by cortical neurons (Cornil et al., 2006; Hojo et al., 2008; Azcoitia et al., 2011). Receptors with high levels of constitutive activity may experience a

reduction in basal activity (i.e., inverse agonist) in response to antagonist (Kenakin, 2006). This may explain the observed inhibitory effects of G-15. Together, variable expression of transducers and endogenous synthesis of GPER ligands may explain the differential response of GPER to G-15 in hippocampal and cortical neurons. The impact of these observations may result in distinct physiological outcomes and future experimental testing of these postulations is warranted.

Different actions of GPER on neuronal activity and cytosolic Ca^{2+} signaling in hippocampal and cortical neurons

The rapid action and signaling of GPER in neurons have been associated with the ability to change neuronal firing activity and/or intracellular messengers such as Ca^{2+} (Altmann et al., 2015; Evans et al., 2016; Rebas et al., 2017). The frequency and patterns of neural activity and Ca^{2+} oscillations are important signaling factors that influence early neuronal development, including growth cone dynamics, axon pathfinding, neurite extension, and synaptic plasticity (Kanemaru et al., 2007; Toth et al., 2016). Here, we found that GPER induced a rapid increase in neuronal firing activity within minutes of E2 and G-1 application in both hippocampal and cortical neurons. Interestingly, GPER significantly increased intracellular Ca^{2+} in hippocampal, but not cortical, neurons. Consistently, E2 has been found to increase cytosolic Ca^{2+} in hippocampal neurons (Wu et al., 2005), while a recent study failed to detect an effect of GPER on cortical Ca^{2+} in neurons, but discovered an effect in astrocytes (Roque and Baltazar, 2019; Roque et al., 2019). GPER also increases cytosolic Ca^{2+} in hypothalamic astrocytes (Kuo et al., 2010). Together, these studies indicate that GPER's role in regulating neuronal excitability and intracellular Ca^{2+} is brain region and cell type dependent.

In addition, the source of Ca^{2+} and Ca^{2+} signaling pathways may be unique to brain regions or cell types. We found that G-1 activity increases cytosolic Ca^{2+} likely via VGCC-mediated extracellular Ca^{2+} entry and PLC-dependent internal Ca^{2+} store release. This is consistent with the finding that G-1 induced cytosolic Ca^{2+} in brain microvascular endothelial cells via L-type VGCCs (Altmann et al., 2015). Interestingly, the increase in cytosolic Ca^{2+} in endothelial cells further activated Ca^{2+}-activated K^{+} channels, contributing to G-1-induced hyperpolarization (Altmann et al., 2015). This is in contrast to the membrane depolarization observed in our study and another with SH-SY5Y cells (Ding et al., 2019). It is important to note that CdCl$_2$ and Ca^{2+}-free solutions used in this study are nonselective blockers and may affect other channel activities, such as K^{+} channels (Stockand et al., 1993; Du et al., 2011) and SOCs. Therefore, the involvement of specific VGCCs and other potential channels such as K^{+}, SOCs, etc. should be further explored using selective blockers and molecular knock-out methods. Nevertheless, the degree of change in neuronal firing activity and/or Ca^{2+} has been tightly associated with developmental processes such as synaptic plasticity (Malenka, 1991; Zamora Chimal and De Schutter, 2018) and axon guidance (Sutherland et al., 2014). Thus, the different

GPER actions and potency on neural activity and Ca^{2+} may contribute to the difference in neurite outgrowth in hippocampal and cortical neurons. Our data indicated that Ca^{2+} release via PLC-IP$_3$ stores may participate in maintaining Ca^{2+} spiking patterns because the amplitude and spiking pattern of Ca^{2+} (Fig. 6E) were drastically reduced in the presence of selective PLC inhibitors. The identification of major signaling pathways associated with GPER allows us to better understand its physiological roles and mechanistic actions during early neuronal development.

GPER expression in hippocampal and cortical neurons or tissues

To test whether GPER expression in hippocampal and cortical neurons may contribute to their distinct physiological effects, we found that GPER is profoundly expressed in both cell types, more richly expressed in the cell body than in neurites, and primarily localized intracellularly. Although we did not find a difference in GPER expression pattern between hippocampal and cortical neurons, our results revealed prevalent subcellular localization of GPER. This agrees with previous results in adult hippocampal (Matsuda et al., 2008) and hypothalamic (Sakamoto et al., 2007) neurons, as well as in COS7 (Monkey kidney fibroblast) cells (Revankar et al., 2005), although plasma membrane localization was found in intact (fixed but not permeabilized) HEK-293 expressing HA-GPER (Filardo et al., 2007). Interestingly, the same study also showed that when HEK cells were permeabilized with Triton X-100, intracellular HA-GPER clusters were found. It is not known whether the observed intracellular localization of GPER in our study is a consequence of permeabilization during immunostaining. However, intracellular localization of GPER and many other GPCRs has been reported and implicated to be associated with receptor biogenesis, posttranslational regulation, and trafficking (Bermak and Zhou, 2001; Mizrachi and Segaloff, 2004; Duvernay et al., 2005; Revankar et al., 2005). Many GPCRs including GPER are intracellularly functional, particularly when their ligands (e.g., steroid hormones) are membrane permeable (Nezhady et al., 2020). Subcellularly, GPER was shown to be localized in cytosolic organelles such as Golgi, endoplasmic reticulum, and other endosome or lysosomal organelles (Gaudet et al., 2015). Intriguingly, previous studies have reported that >30 different GPCRs including GPER were also detected in the nuclei of cells (Gobeil et al., 2006; Boivin et al., 2008; Pupo et al., 2013, 2017; Joyal et al., 2015), where it was shown to be localized to the nucleus of isolated breast cancer-associated fibroblasts (CAFs) and functions as a transcription factor that up-regulates the expression of genes such as c-FOS or CTGF (connective tissue growth factor; Madeo and Maggiolini, 2010; Pupo et al., 2013). Consistently, GPER in our cultured E18 hippocampal and cortical neurons also had nuclear localization (Fig. 7), and other studies found that the GPER protein sequence contains a nuclear localization signal and de-glycosylation of GPER triggers nuclear localization (Pupo et al., 2017).

The existence of nonglycosylated ($\sim$42 kDa) and glycosylated (>42 kDa) GPER proteins was found to correlate with various protein species in immunoblotting studies (de Valdivia et al., 2019). Similarly, in E18 hippocampal and cortical tissues, we observed two protein species with mass sizes of $\sim$42 and 50 kDa. Since our GPER antibody recognizes both protein species, it is not known whether these different protein species are selectively localized in the cytoplasm versus nuclear area in our fluorescence images. Future studies revealing the specific localization of two GPER protein forms in the subcellular structures and their associated functions would be interesting. Regardless of their localization patterns, our qPCR and Western blot data show predominant expression of GPER transcripts and proteins in the cortex compared with the hippocampus. This result is consistent with a previous study showing that GPER mRNA level is more abundant in cortical than hippocampal tissues of both female and male adult rat brains (Hutson et al., 2019). These expression data seem to indicate that the amount of GPER expression does not correlate with the robustness of physiological response it may induce. The physiological effects we observed may instead be determined by the coupling of GPER to different signaling pathways and molecular effectors in hippocampal and cortical neurons.

Distinct transcriptomic regulation by GPER in hippocampal and cortical neurons

Correlating with the distinct outgrowth and Ca^{2+} signaling effects, our RNA sequencing revealed distinct transcriptomic regulation by GPER in hippocampal and cortical neurons, resulting in different gene clustering patterns between treatments in hippocampal and cortical cultures. As shown by unsupervised hierarchical clustering analysis, there was no significant correlation between significantly DE genes as shown by correlation plot analysis and little overlap as shown by Venn diagram analysis. These data indicate that few shared genes and pathways are commonly upregulated or downregulated in both hippocampal and cortical neurons by either E2 or G-1. Importantly, our data clearly demonstrate that E2 and G-1 induced a much stronger transcriptomic regulation of DE genes in hippocampal (1200/159 DE genes) than cortical (157/8 DE genes) cultures, indicating that estrogen and ERs, especially GPER, seem to be more actively engaged in transcriptomic regulation in hippocampal cells at the E18 stage. More interestingly, our hippocampal RNAseq data show transcriptomic enrichment for genes/pathways critically involved in early brain developmental processes such as axonal/dendritic growth and G-protein/protein kinases signaling. The enrichment of DE genes in these early developmental processes supports the neurotrophic effects of G-1/E2 on promoting hippocampal neuritogenesis, neurite outgrowth, and filopodia extensions in our and other studies (Brinton, 1993; Ruiz-Palmero et al., 2011, 2013). Although G-1 and E2 did not promote neuritic development of E18 cortical neurons, our RNA sequencing data indicate a role of E2 in regulating transcripts related to protein translation, chemical

synaptic signaling, and ribosomal and mitochondrial pathways. In addition, G-1 treatment was found to significantly regulate a cysteine desulfurase, mitochondrial-like gene, LOC100911034, which catalyzes the formation of an iron-sulfur (Fe-S) cluster (Poliak et al., 2010) that acts as an essential protein cofactor for many crucial biochemical processes (Patra and Barondeau, 2019). Together, these findings in cortical neurons indicate that, although GPER did not significantly affect early neurite outgrowth, it may play essential roles in regulating biochemical processes or later synaptic events such as chemical synaptic signaling and protein synthesis during synaptic plasticity. In support of this hypothesis, studies have shown that aromatase, a member of the cytochrome P450 superfamily that is responsible for estrogen biosynthesis, is expressed and colocalized with both presynaptic and postsynaptic machinery in cultured mature cortical neurons (Srivastava et al., 2010). This study, together with our RNA sequencing results, suggests an important role for estrogen in later developmental stages, spinogenesis, and plasticity in cortical neurons.

In hippocampal cultures, many DE genes that are significantly regulated by G-1 and/or E2 are related to nervous system development and particularly worthy of discussing here, including genes involved in neurite growth such as *Dpysl5*, *Dpysl3*, and *Gap43*. The *Dpysl5/3* (*dihlikeydropyrimidinase-related protein 5/3*) gene encodes a member of the collapsin response mediator protein (CRMP) family that is highly expressed in the olfactory bulb and hippocampus of developing brains and is involved in axon guidance and neurite outgrowth during neural development (Veyrac et al., 2011; Gong et al., 2016). CRMP members are regulators of voltage-gated Ca^{2+} and Na$^+$ channels (Chew and Khanna, 2018) and hence neuronal activity and activity-dependent neurite outgrowth (Wilson et al., 2014). *Gap43* encodes Gap43, which is a critical component of the axonal growth cone and presynaptic terminal (Strittmatter et al., 1994; Okada et al., 2021). Interestingly, the expression of *Gap43* mRNA in neurons can be modulated by neuronal activity (Caprini et al., 2003; Rosskothen-Kuhl and Illing, 2014). The ability of CRMP and GAP43 to regulate neurite development and activity is intriguing since GPER agonists are found to induce activity changes in hippocampal neurons by the present study. In addition, several genes encoding actin-binding proteins (*Cfl1*, *Pfn1*, *Fscn1*), neurofilament (*Nefm*), and adhesion molecules (*Nrxn2*, *Adgrb2*, and *Cadm4*) are also significantly upregulated by G-1 and E2 or G-1 alone (also see Extended Data Figs. 9-1, 9-2; Hunter et al., 2011; Golan et al., 2013; Duman et al., 2016; Pervolaraki et al., 2019). In addition, the expression of *Cfl1*, *Pfn1*, and *Nrxn2* genes are found to be activity or Ca^{2+} dependent (Neuhoff et al., 2005; Rozic-Kotliroff and Zisapel, 2007; Feuge et al., 2019; Liakath-Ali and Südhof, 2021) and estrogen has been discovered to stimulate the phosphorylation of Cofilin (encoded by *Cfl1* gene), which induces elongation of actin filaments and growth of dendritic spines (Yuen et al., 2011). Furthermore, our RNAseq results also point to GPCR signaling genes specifically altered in hippocampal cultures. For example, both G-1 and E2 treatments increase the expression of

Rangap1 (Ran GTPase activating protein 1) which is involved in Ras signaling (Takeda et al., 2005; Ritterhoff et al., 2016), and of *Gpsm1* (G-protein signaling modulator 1) which is involved in the regulation of $G\alpha_{i/o}$ or $G\beta\gamma$ subunits through GPSM1 binding to GDP-bound $G\alpha$ leading to the release of free $G\beta\gamma$ (Blumer et al., 2012; Oner et al., 2013). $G\beta\gamma$ has been shown to directly inhibit VGCC (Tedford and Zamponi, 2006) or indirectly release Ca^{2+} from internal stores via PLC activation (Boyer et al., 1992; Park et al., 1993; Werry et al., 2003). These effects of $G\beta\gamma$ on cytosol Ca^{2+} may mediate different and opposing effects in different cell types such as in cortical neurons versus glial cells (Roque and Baltazar, 2019; Roque et al., 2019) or hippocampal neurons seen in this study. Future studies on GPER's association with G_s or $G_{i/o}$ as well as their $G\beta\gamma$ signaling in hippocampal and cortical development and physiology would be interesting and important. Lastly, two protein kinase genes, *Camk2b* and *Akt1*, are significantly upregulated by G-1 or E2. Camk2b encodes Ca^{2+}/calmodulin-dependent protein kinase II β (CaMKIIB), which is involved in the regulation of neurite extension and dendritic arborization in developing hippocampal neurons (Wayman et al., 2006; Puram et al., 2011). Since Ca^{2+} is a major determinant for GPER-distinct effects on hippocampal and cortical neurons, a downstream Ca^{2+} effector such as CaMKIIB appears to be an intriguing kinase for future follow-up studies. Furthermore, G-1 (but not E2) treatment significantly increases the expression of *Akt1*, which encodes protein kinase B (PKB) that is involved in multiple functions in neurons via activation of the nuclear factor κB (NF-κB) transcription factor or mammalian target of rapamycin (mTOR) pathways (Bai et al., 2009; Manning and Toker, 2017).

In conclusion, this study identified that GPER plays a more prominent neurotrophic role in the neurite outgrowth of rat E18 hippocampal than cortical neurons. This may arise from the signaling events of GPER that have greater effects on the rapid modulation of neuronal activity and Ca^{2+} oscillations. The resulting change in activity and Ca^{2+} then act as determining signals for downstream gene transcriptomic regulation and morphologic development. Our data also indicates that GPER may regulate neurite outgrowth in hippocampal neurons by actively regulating gene profiles involved in nervous system development, axonal/dendritic growth, and G-protein/kinase signaling. This study identifies several interesting genes and signaling pathways that warrant further research. While our data agreed with previous studies showing a lack of activity or variable effect in response to GPER activation within the cortex, these results do not rule out the important role of GPER in cortical neurons. Rather, we emphasize that the involvement of GPER may depend on developmental period, cell type, or brain region. Identifying these differences and response pathways is crucial for our understanding of estrogen function via GPER in early neuron development or neurodevelopmental disorders.

References

Altmann JB, Yan G, Meeks JF, Abood ME, Brailoiu E, Brailoiu GC (2015) G protein-coupled estrogen receptor-mediated effects on cytosolic calcium and nanomechanics in brain microvascular endothelial cells. J Neurochem 133:629–639.

Altun H, Kurutas EB, Sahin N, Sinir H, Findikli E (2017) Decreased levels of G protein-coupled estrogen receptor in children with autism spectrum disorders. Psychiatry Res 257:67–71.

Amendola J, Woodhouse A, Martin-Eauclaire MF, Goaillard JM (2012) Ca(2)(+)/cAMP-sensitive covariation of I(A) and I(H) voltage dependences tunes rebound firing in dopaminergic neurons. J Neurosci 32:2166–2181.

Azcoitia I, Yague JG, Garcia-Segura LM (2011) Estradiol synthesis within the human brain. Neuroscience 191:139–147.

Bahrami F, Janahmadi M (2013) Antibiotic supplements affect electrophysiological properties and excitability of rat hippocampal pyramidal neurons in primary culture. Iran Biomed J 17:101–106.

Bai D, Ueno L, Vogt PK (2009) Akt-mediated regulation of NFkappaB and the essentialness of NFkappaB for the oncogenicity of PI3K and Akt. Int J Cancer 125:2863–2870.

Basarsky TA, Parpura V, Haydon PG (1994) Hippocampal synaptogenesis in cell culture: developmental time course of synapse formation, calcium influx, and synaptic protein distribution. J Neurosci 14:6402–6411.

Bermak JC, Zhou QY (2001) Accessory proteins in the biogenesis of G protein-coupled receptors. Mol Interv 1:282–287.

Beyer C, Ivanova T, Karolczak M, Küppers E (2002) Cell type-specificity of nonclassical estrogen signaling in the developing midbrain. J Steroid Biochem Mol Biol 81:319–325.

Blumer JB, Oner SS, Lanier SM (2012) Group II activators of G-protein signalling and proteins containing a G-protein regulatory motif. Acta Physiol (Oxf) 204:202–218.

Boivin B, Vaniotis G, Allen BG, Hébert TE (2008) G protein-coupled receptors in and on the cell nucleus: a new signaling paradigm? J Recept Signal Transduct Res 28:15–28.

Bologa CG, Revankar CM, Young SM, Edwards BS, Arterburn JB, Kiselyov AS, Parker MA, Tkachenko SE, Savchuck NP, Sklar LA, Oprea TI, Prossnitz ER (2006) Virtual and biomolecular screening converge on a selective agonist for GPR30. Nat Chem Biol 2:207–212.

Borodinsky LN, Belgacem YH (2016) Crosstalk among electrical activity, trophic factors and morphogenetic proteins in the regulation of neurotransmitter phenotype specification. J Chem Neuroanat 73:3–8.

Bourque M, Morissette M, Di Paolo T (2015) Neuroprotection in Parkinsonian-treated mice via estrogen receptor α activation requires G protein-coupled estrogen receptor 1. Neuropharmacology 95:343–352.

Boyer JL, Waldo GL, Harden TK (1992) Beta gamma-subunit activation of G-protein-regulated phospholipase C. J Biol Chem 267:25451–25456.

Brailoiu E, Dun SL, Brailoiu GC, Mizuo K, Sklar LA, Oprea TI, Prossnitz ER, Dun NJ (2007) Distribution and characterization of estrogen receptor G protein-coupled receptor 30 in the rat central nervous system. J Endocrinol 193:311–321.

Brinton RD (1993) 17beta-estradiol induction of filopodial growth in cultured hippocampal neurons within minutes of exposure. Mol Cell Neurosci 4:36–46.

Brinton RD, Tran J, Proffitt P, Montoya M (1997) 17 beta-Estradiol enhances the outgrowth and survival of neocortical neurons in culture. Neurochem Res 22:1339–1351.

Broughton BR, Brait VH, Kim HA, Lee S, Chu HX, Gardiner-Mann CV, Guida E, Evans MA, Miller AA, Arumugam TV, Drummond GR, Sobey CG (2014) Sex-dependent effects of G protein-coupled estrogen receptor activity on outcome after ischemic stroke. Stroke 45:835–841.

Caprini M, Gomis A, Cabedo H, Planells-Cases R, Belmonte C, Viana F, Ferrer-Montiel A (2003) GAP43 stimulates inositol trisphosphate-mediated calcium release in response to hypotonicity. EMBO J 22:3004–3014.

Carmeci C, Thompson DA, Ring HZ, Francke U, Weigel RJ (1997) Identification of a gene (GPR30) with homology to the G-protein-coupled receptor superfamily associated with estrogen receptor expression in breast cancer. Genomics 45:607–617.

Chen H, Boutros PC (2011) VennDiagram: a package for the generation of highly-customizable Venn and Euler diagrams in R. BMC Bioinformatics 12:35.

Chew LA, Khanna R (2018) CRMP2 and voltage-gated ion channels: potential roles in neuropathic pain. Neuronal Signal 2: NS20170220.

Chin G, El-Sherif Y, Jayman F, Estephan R, Wieraszko A, Banerjee P (2003) Appearance of voltage-gated calcium channels following overexpression of ATPase II cDNA in neuronal HN2 cells. Brain Res Mol Brain Res 117:109–115.

Cornil CA, Ball GF, Balthazart J (2006) Functional significance of the rapid regulation of brain estrogen action: where do the estrogens come from? Brain Res 1126:2–26.

Côté M, Bourque M, Poirier AA, Aubé B, Morissette M, Di Paolo T, Soulet D (2015) GPER1-mediated immunomodulation and neuroprotection in the myenteric plexus of a mouse model of Parkinson's disease. Neurobiol Dis 82:99–113.

Dascal N, Snutch TP, Lübbert H, Davidson N, Lester HA (1986) Expression and modulation of voltage-gated calcium channels after RNA injection in *Xenopus* oocytes. Science 231:1147–1150.

de Valdivia EG, Broselid S, Kahn R, Olde B, Leeb-Lundberg LMF (2017) G protein-coupled estrogen receptor 1 (GPER1)/GPR30 increases ERK1/2 activity through PDZ motif-dependent and -independent mechanisms. J Biol Chem 292:9932–9943.

de Valdivia EG, Sandén C, Kahn R, Olde B, Leeb-Lundberg LMF (2019) Human G protein-coupled receptor 30 is N-glycosylated and N-terminal domain asparagine 44 is required for receptor structure and activity. Bioscience Rep 39:BSR20182436.

De Waard M, Liu H, Walker D, Scott VE, Gurnett CA, Campbell KP (1997) Direct binding of G-protein betagamma complex to voltage-dependent calcium channels. Nature 385:446–450.

Dehorter N, Vinay L, Hammond C, Ben-Ari Y (2012) Timing of developmental sequences in different brain structures: physiological and pathological implications. Eur J Neurosci 35:1846–1856.

Dennis MK, Field AS, Burai R, Ramesh C, Petrie WK, Bologa CG, Oprea TI, Yamaguchi Y, Hayashi S, Sklar LA, Hathaway HJ, Arterburn JB, Prossnitz ER (2011) Identification of a GPER/GPR30 antagonist with improved estrogen receptor counterselectivity. J Steroid Biochem Mol Biol 127:358–366.

Ding X, Gao T, Gao P, Meng Y, Zheng Y, Dong L, Luo P, Zhang G, Shi X, Rong W (2019) Activation of the G protein-coupled estrogen receptor elicits store calcium release and phosphorylation of the mu-opioid receptors in the human neuroblastoma SH-SY5Y cells. Front Neurosci 13:1351.

Dowle M, Srinivasan A (2019) Data.table: extension of 'data.frame'. R package version 1.14.2. Retrieved from https://CRAN.R-project.org/package=data.table.

Du CL, Wang LH, Jiang N, Huang XH (2011) Effect of heavy metal cadmium ion on outward potassium channel in cell. Acta Chim Sinica 69:601–604.

Duman JG, Tu YK, Tolias KF (2016) Emerging roles of BAI adhesion-GPCRs in synapse development and plasticity. Neural Plast 2016:8301737.

Duvernay MT, Filipeanu CM, Wu G (2005) The regulatory mechanisms of export trafficking of G protein-coupled receptors. Cell Signal 17:1457–1465.

Edelstein A, Amodaj N, Hoover K, Vale R, Stuurman N (2010) Computer control of microscopes using μManager. Curr Protoc Mol Biol 92:14.20.11–14.20.17.

Evans NJ, Bayliss AL, Reale V, Evans PD (2016) Characterisation of signalling by the endogenous GPER1 (GPR30) receptor in an embryonic mouse hippocampal cell line (mHippoE-18). PLoS One 11: e0152138.

Feuge J, Scharkowski F, Michaelsen-Preusse K, Korte M (2019) FMRP modulates activity-dependent spine plasticity by binding cofilin1 mRNA and regulating localization and local translation. Cereb Cortex 29:5204–5216.

Filardo EJ, Quinn JA, Frackelton AR Jr, Bland KI (2002) Estrogen action via the G protein-coupled receptor, GPR30: stimulation of adenylyl cyclase and cAMP-mediated attenuation of the epidermal growth factor receptor-to-MAPK signaling axis. Mol Endocrinol 16:70–84.

Filardo E, Quinn J, Pang Y, Graeber C, Shaw S, Dong J, Thomas P (2007) Activation of the novel estrogen receptor G protein-coupled receptor 30 (GPR30) at the plasma membrane. Endocrinology 148:3236–3245.

Gaudet HM, Cheng SB, Christensen EM, Filardo EJ (2015) The G-protein coupled estrogen receptor, GPER: the inside and inside-out story. Mol Cell Endocrinol 418:207–219.

Gobeil F, Fortier A, Zhu T, Bossolasco M, Leduc M, Grandbois M, Heveker N, Bkaily G, Chemtob S, Barbaz D (2006) G-protein-coupled receptors signalling at the cell nucleus: an emerging paradigm. Can J Physiol Pharmacol 84:287–297.

Gogos A, Sbisa AM, Sun J, Gibbons A, Udawela M, Dean B (2015) A role for estrogen in schizophrenia: clinical and preclinical findings. Int J Endocrinol 2015:615356.

Golan N, Kartvelishvily E, Spiegel I, Salomon D, Sabanay H, Rechav K, Vainshtein A, Frechter S, Maik-Rachline G, Eshed-Eisenbach Y, Momoi T, Peles E (2013) Genetic deletion of Cadm4 results in myelin abnormalities resembling Charcot-Marie-Tooth neuropathy. J Neurosci 33:10950–10961.

Gong X, Tan M, Gao Y, Chen K, Guo G (2016) CRMP-5 interacts with actin to regulate neurite outgrowth. Mol Med Rep 13:1179–1185.

Graves S, Piepho HP, Selzer L (2015) Multcompview: visualizations of paired comparisons. R Package Version 0.1-8. Retrieved from https://cran.r-project.org/package=multcompView.

Green S, Walter P, Kumar V, Krust A, Bornert JM, Argos P, Chambon P (1986) Human oestrogen receptor cDNA: sequence, expression and homology to v-erb-A. Nature 320:134–139.

Hao J, Bao X, Jin B, Wang X, Mao Z, Li X, Wei L, Shen D, Wang JL (2015) Ca2+ channel subunit α 1D promotes proliferation and migration of endometrial cancer cells mediated by 17β-estradiol via the G protein-coupled estrogen receptor. FASEB J 29:2883–2893.

Hazell GGJ, Yao ST, Roper JA, Prossnitz ER, O'Carroll AM, Lolait SJ (2009) Localisation of GPR30, a novel G protein-coupled oestrogen receptor, suggests multiple functions in rodent brain and peripheral tissues. J Endocrinol 202:223–236.

Hojo Y, Murakami G, Mukai H, Higo S, Hatanaka Y, Ogiue-Ikeda M, Ishii H, Kimoto T, Kawato S (2008) Estrogen synthesis in the brain–role in synaptic plasticity and memory. Mol Cell Endocrinol 290:31–43.

Hothorn T, Bretz F, Westfall P (2019) Simultaneous inference in general parametric models. Biom J 50:346–363.

Hunter PR, Nikolaou N, Odermatt B, Williams PR, Drescher U, Meyer MP (2011) Localization of Cadm2a and Cadm3 proteins during development of the zebrafish nervous system. J Comp Neurol 519:2252–2270.

Hutson DD, Gurrala R, Ogola BO, Zimmerman MA, Mostany R, Satou R, Lindsey SH (2019) Estrogen receptor profiles across tissues from male and female *Rattus norvegicus*. Biol Sex Differ 10:4–4.

Imaninezhad M, Pemberton K, Xu F, Kalinowski K, Bera R, Zustiak SP (2018) Directed and enhanced neurite outgrowth following exogenous electrical stimulation on carbon nanotube-hydrogel composites. J Neural Eng 15:056034–056034.

Ji Y, Han Z, Shao L, Zhao Y (2016) Ultrasound-targeted microbubble destruction of calcium channel subunit α 1D siRNA inhibits breast cancer via G protein-coupled receptor 30. Oncol Rep 36:1886–1892.

Jin W, Lo TM, Loh HH, Thayer SA (1994) U73122 inhibits phospholipase C-dependent calcium mobilization in neuronal cells. Brain Res 642:237–243.

Joyal JS, Bhosle VK, Chemtob S (2015) Subcellular G-protein coupled receptor signaling hints at greater therapeutic selectivity. Expert Opin Ther Targets 19:717–721.

Kajta M, Beyer C (2003) Cellular strategies of estrogen-mediated neuroprotection during brain development. Endocrine 21:3–9.

Kanemaru K, Okubo Y, Hirose K, Iino M (2007) Regulation of neurite growth by spontaneous Ca2+ oscillations in astrocytes. J Neurosci 27:8957–8966.

Kato D, Wake H (2019) Activity-dependent myelination. Adv Exp Med Biol 1190:43–51.

Kenakin T (2006) Testing for inverse agonism with constitutive receptor systems. Curr Protoc Pharmacol Chapter 9:Unit9 5.

Kolde R (2019) Pheatmap: pretty heatmaps. R package version 1.0.12. Retrieved from https://CRAN.R-project.org/package=pheatmap.

Konkle AT, McCarthy MM (2011) Developmental time course of estradiol, testosterone, and dihydrotestosterone levels in discrete regions of male and female rat brain. Endocrinology 152:223–235.

Kuiper GG, Enmark E, Pelto-Huikko M, Nilsson S, Gustafsson JA (1996) Cloning of a novel receptor expressed in rat prostate and ovary. Proc Natl Acad Sci U S A 93:5925–5930.

Kumar A, Foster TC (2020) G protein-coupled estrogen receptor: rapid effects on hippocampal-dependent spatial memory and synaptic plasticity. Front Endocrinol (Lausanne) 11:385.

Kuo J, Hamid N, Bondar G, Prossnitz ER, Micevych P (2010) Membrane estrogen receptors stimulate intracellular calcium release and progesterone synthesis in hypothalamic astrocytes. J Neurosci 30:12950–12957.

Kvingedal AM, Smeland EB (1997) A novel putative G-protein-coupled receptor expressed in lung, heart and lymphoid tissue. FEBS Lett 407:59–62.

Leavitt AM, Watchko JF, Bennett FC, Folsom RC (1987) Neurodevelopmental outcome following persistent pulmonary hypertension of the neonate. J Perinatol 7:288–291.

Leclerc C, Néant I, Moreau M (2012) The calcium: an early signal that initiates the formation of the nervous system during embryogenesis. Front Mol Neurosci 5:3.

Lee BJ, Yang CH, Lee SY, Lee SH, Kim Y, Ho WK (2022) Voltage-gated calcium channels contribute to spontaneous glutamate release directly via nanodomain coupling or indirectly via calmodulin. Prog Neurobiol 208:102182.

Lenth R (2019) Emmeans: estimated marginal means, aka Least-Squares Means. R package version 1.7.5. Retrieved from https://CRAN.R-project.org/package=emmeans.

Li Q, Sullivan NR, McAllister CE, Van de Kar LD, Muma NA (2013) Estradiol accelerates the effects of fluoxetine on serotonin 1A receptor signaling. Psychoneuroendocrinology 38:1145–1157.

Liakath-Ali K, Südhof TC (2021) The perils of navigating activity-dependent alternative splicing of neurexins. Front Mol Neurosci 14:659681.

Luhmann HJ, Sinning A, Yang JW, Reyes-Puerta V, Stüttgen MC, Kirischuk S, Kilb W (2016) Spontaneous neuronal activity in developing neocortical networks: from single cells to large-scale interactions. Front Neural Circuits 10:40–40.

Madeo A, Maggiolini M (2010) Nuclear alternate estrogen receptor GPR30 mediates 17 beta-estradiol-induced gene expression and migration in breast cancer-associated fibroblasts. Cancer Res 70:6036–6046.

Malenka RC (1991) The role of postsynaptic calcium in the induction of long-term potentiation. Mol Neurobiol 5:289–295.

Manning BD, Toker A (2017) AKT/PKB signaling: navigating the network. Cell 169:381–405.

Martínez Damonte V, Rodríguez SS, Raingo J (2018) Growth hormone secretagogue receptor constitutive activity impairs voltage-gated calcium channel-dependent inhibitory neurotransmission in hippocampal neurons. J Physiol 596:5415–5428.

Matsuda K, Sakamoto H, Mori H, Hosokawa K, Kawamura A, Itose M, Nishi M, Prossnitz ER, Kawata M (2008) Expression and intracellular distribution of the G protein-coupled receptor 30 in rat hippocampal formation. Neurosci Lett 441:94–99.

McAllister CE, Creech RD, Kimball PA, Muma NA, Li Q (2012) GPR30 is necessary for estradiol-induced desensitization of 5-HT1A receptor signaling in the paraventricular nucleus of the rat hypothalamus. Psychoneuroendocrinology 37:1248–1260.

McAllister CE, Mi Z, Mure M, Li Q, Muma NA (2014) GPER1 stimulation alters posttranslational modification of RGSz1 and induces desensitization of 5-HT1A receptor signaling in the rat hypothalamus. Neuroendocrinology 100:228–239.

McCarthy MM (2008) Estradiol and the developing brain. Physiol Rev 88:91–124.

McCarthy MM (2016) Sex differences in the developing brain as a source of inherent risk. Dialogues Clin Neurosci 18:361–372.

Meijering E, Jacob M, Sarria JCF, Steiner P, Hirling H, Unser M (2004) Design and validation of a tool for neurite tracing and analysis in fluorescence microscopy images. Cytometry A 58:167–176.

Mersman B, Zaidi W, Syed NI, Xu F (2020) Taurine promotes neurite outgrowth and synapse development of both vertebrate and invertebrate central neurons. Front Synaptic Neurosci 12:29.

Miranda RC, Sohrabji F, Toran-Allerand D (1994) Interactions of estrogen with the neurotrophins and their receptors during neural development. Horm Behav 28:367–375.

Mizrachi D, Segaloff DL (2004) Intracellularly located misfolded glycoprotein hormone receptors associate with different chaperone proteins than their cognate wild-type receptors. Mol Endocrinol 18:1768–1777.

Murata T, Dietrich HH, Xiang C, Dacey RG Jr (2013) G protein-coupled estrogen receptor agonist improves cerebral microvascular function after hypoxia/reoxygenation injury in male and female rats. Stroke 44:779–785.

Neuhoff H, Sassoè-Pognetto M, Panzanelli P, Maas C, Witke W, Kneussel M (2005) The actin-binding protein profilin I is localized at synaptic sites in an activity-regulated manner. Eur J Neurosci 21:15–25.

Nezhady MAM, Rivera JC, Chemtob S (2020) Location bias as emerging paradigm in GPCR biology and drug discovery. Iscience 23:101643.

Okada M, Kawagoe Y, Sato Y, Nozumi M, Ishikawa Y, Tamada A, Yamazaki H, Sekino Y, Kanemura Y, Shinmyo Y, Kawasaki H, Kaneko N, Sawamoto K, Fujii Y, Igarashi M (2021) Phosphorylation of GAP-43 T172 is a molecular marker of growing axons in a wide range of mammals including primates. Mol Brain 14:66.

Oner SS, Blumer JB, Lanier SM (2013) Group II activators of G-protein signaling: monitoring the interaction of Gα with the G-protein regulatory motif in the intact cell. Methods Enzymol 522:153–167.

Pacifici M, Peruzzi F (2012) Isolation and culture of rat embryonic neural cells: a quick protocol. J Vis Exp (63):e3965.

Park D, Jhon DY, Lee CW, Lee KH, Rhee SG (1993) Activation of phospholipase C isozymes by G protein beta gamma subunits. J Biol Chem 268:4573–4576.

Patra S, Barondeau DP (2019) Mechanism of activation of the human cysteine desulfurase complex by frataxin. Proc Natl Acad Sci U S A 116:19421–19430.

Pemberton K, Mersman B, Xu F (2018) Using ImageJ to assess neurite outgrowth in mammalian cell cultures: research data quantification exercises in undergraduate neuroscience lab. J Undergrad Neurosci Educ 16:A186–A194.

Pervolaraki E, Tyson AL, Pibiri F, Poulter SL, Reichelt AC, Rodgers RJ, Clapcote SJ, Lever C, Andreae LC, Dachtler J (2019) The within-subject application of diffusion tensor MRI and CLARITY reveals brain structural changes in Nrxn2 deletion mice. Mol Autism 10:8.

Poliak P, Van Hoewyk D, Oborník M, Zíková A, Stuart KD, Tachezy J, Pilon M, Lukes J (2010) Functions and cellular localization of cysteine desulfurase and selenocysteine lyase in Trypanosoma brucei. FEBS J 277:383–393.

Prada J, Sasi M, Martin C, Jablonka S, Dandekar T, Blum R (2018) An open source tool for automatic spatiotemporal assessment of calcium transients and local 'signal-close-to-noise' activity in calcium imaging data. PLoS Comput Biol 14:e1006054.

Prakriya M, Lewis RS (2015) Store-operated calcium channels. Physiol Rev 95:1383–1436.

Proft J, Weiss N (2015) G protein regulation of neuronal calcium channels: back to the future. Mol Pharmacol 87:890–906.

Pupo M, Vivacqua A, Perrotta I, Pisano A, Aquila S, Abonante S, Gasperi-Campani A, Pezzi V, Maggiolini M (2013) The nuclear localization signal is required for nuclear GPER translocation and function in breast cancer-associated fibroblasts (CAFs). Mol Cell Endocrinol 376:23–32.

Pupo M, Bodmer A, Berto M, Maggiolini M, Dietrich PY, Picard D (2017) A genetic polymorphism repurposes the G-protein coupled and membrane-associated estrogen receptor GPER to a transcription factor-like molecule promoting paracrine signaling between stroma and breast carcinoma cells. Oncotarget 8:46728–46744.

Puram SV, Kim AH, Ikeuchi Y, Wilson-Grady JT, Merdes A, Gygi SP, Bonni A (2011) A CaMKIIβ signaling pathway at the centrosome regulates dendrite patterning in the brain. Nat Neurosci 14:973–983.

Raudvere U, Kolberg L, Kuzmin I, Arak T, Adler P, Peterson H, Vilo J (2019) g: profiler: a web server for functional enrichment analysis and conversions of gene lists (2019 update). Nucleic Acids Res 47: W191–W198.

Rebas E, Radzik T, Boczek T, Zylinska L (2017) Calcium-engaged mechanisms of nongenomic action of neurosteroids. Curr Neuropharmacol 15:1174–1191.

Revankar CM, Cimino DF, Sklar LA, Arterburn JB, Prossnitz ER (2005) A transmembrane intracellular estrogen receptor mediates rapid cell signaling. Science 307:1625–1630.

Ritterhoff T, Das H, Hofhaus G, Schröder RR, Flotho A, Melchior F (2016) The RanBP2/RanGAP1*SUMO1/Ubc9 SUMO E3 ligase is a disassembly machine for Crm1-dependent nuclear export complexes. Nat Commun 7:11482.

Roque C, Baltazar G (2019) G protein-coupled estrogen receptor 1 (GPER) activation triggers different signaling pathways on neurons and astrocytes. Neural Regen Res 14:2069–2070.

Roque C, Mendes-Oliveira J, Baltazar G (2019) G protein-coupled estrogen receptor activates cell type-specific signaling pathways in cortical cultures: relevance to the selective loss of astrocytes. J Neurochem 149:27–40.

Rosenberg SS, Spitzer NC (2011) Calcium signaling in neuronal development. Cold Spring Harb Perspect Biol 3:a004259.

Rosskothen-Kuhl N, Illing RB (2014) Gap43 transcription modulation in the adult brain depends on sensory activity and synaptic cooperation. PLoS One 9:e92624.

Rozic-Kotliroff G, Zisapel N (2007) Ca2+ -dependent splicing of neurexin IIalpha. Biochem Biophys Res Commun 352:226–230.

Rstudio T (2015) RStudio: integrated development for R. Boston: RStudio, Inc.

Ruiz-Palmero I, Simon-Areces J, Garcia-Segura LM, Arevalo MA (2011) Notch/neurogenin 3 signalling is involved in the neuritogenic actions of oestradiol in developing hippocampal neurones. J Neuroendocrinol 23:355–364.

Ruiz-Palmero I, Hernando M, Garcia-Segura LM, Arevalo MA (2013) G protein-coupled estrogen receptor is required for the neuritogenic mechanism of 17β-estradiol in developing hippocampal neurons. Mol Cell Endocrinol 372:105–115.

Ryu AH, Eckalbar WL, Kreimer A, Yosef N, Ahituv N (2017) Use antibiotics in cell culture with caution: genome-wide identification of antibiotic-induced changes in gene expression and regulation. Sci Rep 7:7533–7533.

Sahin N, Altun H, Kurutaş EB, Fındıklı E (2018) Evaluation of estrogen and G protein-coupled estrogen receptor 1 (GPER) levels in drug-naïve patients with attention deficit hyperactivity disorder (ADHD). Bosn J Basic Med Sci 18:126–131.

Sakamoto H, Matsuda K, Hosokawa K, Nishi M, Morris JF, Prossnitz ER, Kawata M (2007) Expression of G protein-coupled receptor-30, a g protein-coupled membrane estrogen receptor, in oxytocin neurons of the rat paraventricular and supraoptic nuclei. Endocrinology 148:5842–5850.

Schindelin J, Arganda-Carreras I, Frise E, Kaynig V, Longair M, Pietzsch T, Preibisch S, Rueden C, Saalfeld S, Schmid B, Tinevez J-Y, White DJ, Hartenstein V, Eliceiri K, Tomancak P, Cardona A (2012) Fiji: an open-source platform for biological-image analysis. Nat Methods 9:676–682.

Shi Y, Liu X, Zhu P, Li J, Sham KW, Cheng SH, Li S, Zhang Y, Cheng CH, Lin H (2013) G-protein-coupled estrogen receptor 1 is involved in brain development during zebrafish (Danio rerio) embryogenesis. Biochem Biophys Res Commun 435:21–27.

Signorell A, et al. (2019) DescTools: tools for descriptive statistics. R package version 0.99.30. Retrieved from https://cran.r-project.org/package=DescTools.

Slowikowski K (2020) Ggrepel: automatically position non-overlapping text labels with 'ggplot2'. R package version 0.9.1. Retrieved from https://CRAN.R-project.org/package=ggrepel.

Smrcka AV (2008) G protein β γ subunits: central mediators of G protein-coupled receptor signaling. Cell Mol Life Sci 65:2191–2214.

Spitzer NC (2006) Electrical activity in early neuronal development. Nature 444:707–712.

Srivastava DP, Woolfrey KM, Woolfrey K, Jones KA, Shum CY, Lash LL, Swanson GT, Penzes P (2008) Rapid enhancement of two-step wiring plasticity by estrogen and NMDA receptor activity. Proc Natl Acad Sci U S A 105:14650–14655.

Srivastava DP, Woolfrey KM, Liu F, Brandon NJ, Penzes P (2010) Estrogen receptor ss activity modulates synaptic signaling and structure. J Neurosci 30:13454–13460.

Stockand J, Sultan A, Molony D, DuBose T Jr, Sansom S (1993) Interactions of cadmium and nickel with K channels of vascular smooth muscle. Toxicol Appl Pharmacol 121:30–35.

Strittmatter SM, Igarashi M, Fishman MC (1994) GAP-43 amino terminal peptides modulate growth cone morphology and neurite outgrowth. J Neurosci 14:5503–5513.

Sutherland DJ, Pujic Z, Goodhill GJ (2014) Calcium signaling in axon guidance. Trends Neurosci 37:424–432.

Takeda E, Hieda M, Katahira J, Yoneda Y (2005) Phosphorylation of RanGAP1 stabilizes its interaction with Ran and RanBP1. Cell Struct Funct 30:69–80.

Takenouchi T, Ogihara K, Sato M, Kitani H (2005) Inhibitory effects of U73122 and U73343 on Ca2+ influx and pore formation induced by the activation of P2X7 nucleotide receptors in mouse microglial cell line. Biochim Biophys Acta 1726:177–186.

Tang L, Zheng S, Wang Y, Li F, Bao M, Zeng J, Xiang J, Luo H, Li J (2017) Rs4265085 in GPER1 gene increases the risk for unexplained recurrent spontaneous abortion in Dai and Bai ethnic groups in China. Reprod Biomed Online 34:399–405.

Taylor CW (2017) Regulation of IP3 receptors by cyclic AMP. Cell Calcium 63:48–52.

Team RC (2017) R: a language and environment for statistical computing. Vienna: R Foundation for Statistical Computing.

Tedford HW, Zamponi GW (2006) Direct G protein modulation of Cav2 calcium channels. Pharmacol Rev 58:837–862.

Tian Z, Wang Y, Zhang N, Guo YY, Feng B, Liu SB, Zhao MG (2013) Estrogen receptor GPR30 exerts anxiolytic effects by maintaining the balance between GABAergic and glutamatergic transmission in the basolateral amygdala of ovariectomized mice after stress. Psychoneuroendocrinology 38:2218–2233.

Toth AB, Shum AK, Prakriya M (2016) Regulation of neurogenesis by calcium signaling. Cell Calcium 59:124–134.

Tredway TL, Guo JZ, Chiappinelli VA (1999) N-type voltage-dependent calcium channels mediate the nicotinic enhancement of GABA release in chick brain. J Neurophysiol 81:447–454.

Uezono Y, Kaibara M, Murasaki O, Taniyama K (2004) Involvement of G protein betagamma-subunits in diverse signaling induced by G (i/o)-coupled receptors: study using the Xenopus oocyte expression system. Am J Physiol Cell Physiol 287:C885–894.

Veyrac A, Reibel S, Sacquet J, Mutin M, Camdessanche J-P, Kolattukudy P, Honnorat J, Jourdan F (2011) CRMP5 regulates generation and survival of newborn neurons in olfactory and hippocampal neurogenic areas of the adult mouse brain. PLoS One 6: e23721-e23721.

Walter AM, Böhme MA, Sigrist SJ (2018) Vesicle release site organization at synaptic active zones. Neurosci Res 127:3–13.

Walter P, Green S, Greene G, Krust A, Bornert JM, Jeltsch JM, Staub A, Jensen E, Scrace G, Waterfield M (1985) Cloning of the human estrogen receptor cDNA. Proc Natl Acad Sci U S A 82:7889–7893.

Wayman GA, Impey S, Marks D, Saneyoshi T, Grant WF, Derkach V, Soderling TR (2006) Activity-dependent dendritic arborization mediated by CaM-kinase I activation and enhanced CREB-dependent transcription of Wnt-2. Neuron 50:897–909.

Werry TD, Wilkinson GF, Willars GB (2003) Mechanisms of cross-talk between G-protein-coupled receptors resulting in enhanced release of intracellular Ca2+. Biochem J 374:281–296.

Wickham H (2016) Plyr: tools for splitting, applying and combining data. R package version 1.8.4. Retrieved from http://CRAN.R-project.org/package=ncdf4.

Wickham H (2017) Tidyverse: easily install and load the 'tidyverse'. R package version 1.2.1. Retrieved from https://CRAN.R-project.org/package=tidyverse.

Wickham H, Bryan J (2019) Readxl: read excel files. R Package Version 1.3.1. Retrieved from https://CRAN.R-project.org/package=readxl.

Wickham H, François R, Henry L, Müller K (2019) Dplyr: a grammar of data manipulation. R package version 1.0.9. Retrieved from https://CRAN.R-project.org/package=dplyr.

Wilson SM, Moutal A, Melemedjian OK, Wang Y, Ju W, François-Moutal L, Khanna M, Khanna R (2014) The functionalized amino acid (S)-Lacosamide subverts CRMP2-mediated tubulin polymerization to prevent constitutive and activity-dependent increase in neurite outgrowth. Front Cell Neurosci 8:196.

Wu TW, Wang JM, Chen S, Brinton RD (2005) 17Beta-estradiol induced Ca2+ influx via L-type calcium channels activates the Src/ERK/cyclic-AMP response element binding protein signal pathway and BCL-2 expression in rat hippocampal neurons: a potential initiation mechanism for estrogen-induced neuroprotection. Neuroscience 135:59–72.

Xie Y (2019) Knitr: a general-purpose package for dynamic report generation in R. R package version 1.39. Retrieved from https://CRAN.R-project.org/package=knitr.

Yuen GS, McEwen BS, Akama KT (2011) LIM kinase mediates estrogen action on the actin depolymerization factor Cofilin. Brain Res 1379:44–52.

Zamora Chimal CG, De Schutter E (2018) Ca(2+) requirements for long-term depression are frequency sensitive in Purkinje cells. Front Mol Neurosci 11:438.